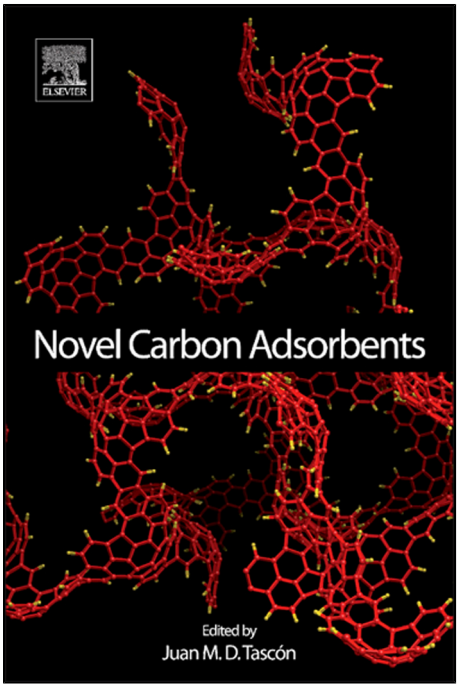

From M. Thommes, K.A. Cychosz, A.V. Neimark, Advanced Physical Adsorption Characterization of Nanoporous Carbons, in: J.M.D. Tascon, Novel Carbon Adsorbents, Elsevier Ltd, 2012, pp. 107–145.
ISBN: 9780080977447

Chapter 4

Advanced Physical Adsorption Characterization of Nanoporous Carbons

Matthias Thommes and Katie A. Cychosz
Quantachrome Instruments, Boynton Beach, FL, USA

Alexander V. Neimark
Rutgers University, Department of Chemical and Biochemical Engineering, Piscataway, NJ, USA

Chapter Outline

4.1. INTRODUCTION

A proper characterization of the textural properties of nanoporous carbons (e.g. activated carbon, carbon aerogels, ordered mesoporous carbons, nanotubes, and

Novel Carbon Adsorbents. DOI: 10.1016/B978-0-08-097744-7.00004-1

Novel Carbon Adsorbents, First Edition, 2012, 107–145

nanohorns) is crucial for a better understanding of their behavior in important industrial applications including separation, gas and energy storage, batteries, and many others [1–5]. Major advancements in materials characterization and practical utilization are related to the progress made in the development of various experimental techniques such as gas adsorption, X-ray diffraction (XRD), small-angle X-ray and neutron scattering (SAXS and SANS), mercury porosimetry, electron microscopy (scanning and transmission), thermoporometry, NMR methods, and others. Each method has a limited length scale of applicability for pore-size analysis and an overview of different methods for pore-size characterization and their application range was given by the International Union of Pure and Applied Chemistry (IUPAC) [6]. However, among all these methods, gas adsorption (i.e. physical adsorption) is still the most popular one because it allows for assessing a wide range of pore sizes (from 0.35 nm up to 100 nm). Furthermore, gas adsorption techniques are convenient to use and less cost intensive than some of the other methods.

Physisorption (physical adsorption) occurs whenever a gas (the adsorptive) is brought into contact with a solid surface (the adsorbent). The matter in the adsorbed state is known as the adsorbate, as distinct from the adsorptive, which is the gas or vapor to be adsorbed. The forces involved in physisorption always include the long-range London dispersion forces and the short-range intermolecular repulsion. These combined forces give rise to nonspecific molecular interactions. Physisorption in porous materials is governed by the interplay between the strength of fluid–wall and fluid–fluid interactions as well as the effects of confined pore space on the state and thermodynamic stability of fluids in narrow pores [7–12]. This is also reflected in the shape or type of the adsorption isotherm. IUPAC has published a classification of six types of adsorption isotherms and proposed to classify pores by their internal pore width (the pore width defined as the diameter in the case of cylindrical and spherical pores and as the distance between opposite walls in case of slit pores) [13]. According to their diameter, the pores are divided into three groups: micropores of width less than 2 nm, mesopores of width between 2 and 50 nm, and macropores of width greater than 50 nm. Micro- and mesopores are often collectively referred to as nanopores. The micropore range is often further subdivided into ultramicropores (pores smaller than 0.7 nm) and supermicropores (pores from 0.7 to 2 nm). As indicated, the pore size is generally specified as the internal pore width, although for mesopores it has been customary to refer to the pore radius (or pore diameter). Of course, such terms have a precise meaning only when the pore shape is properly defined. Furthermore, the internal or effective pore width must not be confused with the distance between the centers of surface atoms (the outer atoms of solid in the opposite walls of a pore), which determines the pore geometry in molecular level theries and simulations. According to [1], the pore morphology describes geometrical shape and structure of the pores including pore width and volume as well as the nature of the pore walls. On the other hand, pore topology describes how the

pores are arranged and the connectivity of pores. It should be noted that a new IUPAC task group has been formed in 2010 which focuses on revising the 1985 recommendations (for more information, see http://www.iupac.org/web/ins/2010-009-1-100).

The recent advances in physical adsorption characterization (for reviews, see for instance [10–12]) are, to a large extent, related to (i) discovery of novel ordered mesoporous materials (e.g. M41S materials), which exhibit a uniform pore size with periodically ordered structure and can therefore be used as model adsorbents to test the theories of gas adsorption; (ii) carefully performed adsorption experiments coupled with complimentary experimental techniques; (iii) development and application of microscopic approaches such as the density functional theory (DFT) of inhomogeneous fluids, as well as methods based on molecular simulation. These modern theoretical and computational methods, which are based on the statistical mechanics of nanophases, describe the configuration of adsorbed fluid (the adsorbate) on a molecular level. It has been shown that the application of DFT methods allows one to obtain reliable pore-size distributions over the complete range of micro- and mesopores. The methods for pore-size analysis based on DFT and molecular simulation are now widely used; they are featured in ISO standard ISO 15901-3 and are commercially available for many important adsorptive/adsorbent systems. The DFT methods include hybrid methods, which assume different pore geometries for the micro- and mesopore size ranges, as found in materials with hierarchical pore structures. More recent advances include the development of quenched solid density functional theory (QSDFT), which quantitatively takes into account the surface geometrical inhomogeneity characterized by a roughness parameter. It has been demonstrated that this novel method significantly improves the accuracy of the pore-size distribution calculations for many micro- and mesoporous carbon materials [14–16].

Within this context, this chapter reviews some important aspects of applying gas adsorption for the textural characterization of micro- and mesoporous carbons, but it should not be considered a comprehensive review. Rather, it discusses important aspects of surface area and pore-size analysis of porous carbons. We address briefly some experimental aspects, focus on adsorption mechanisms in micro- and mesoporous carbons, and then discuss the methods of pore-size/volume characterization on selected examples.

4.2. EXPERIMENTAL ASPECTS

4.2.1. General Comments

The adsorption isotherm, which represents the adsorbed gas amount as a function of pressure at constant temperature, can be obtained by volumetric (manometric) and gravimetric methods, carrier gas and calorimetric techniques, nuclear resonance, as well as by a combination of calorimetric and

impedance spectroscopic measurements (for an overview, see [7–9]). However, the most frequently used methods are the volumetric (manometric) and gravimetric methods. The gravimetric method is based on a sensitive microbalance and a pressure gauge. The adsorbed amount can be measured directly, but a pressure-dependent buoyancy correction is necessary. The gravimetric method is convenient to use for the study of adsorption not too far from room temperature. The volumetric method is recommended to measure adsorption of nitrogen, argon, and krypton at cryogenic temperatures, i.e. the temperatures of liquid nitrogen (77 K) and argon (87 K), which are primarily used for surface area and pore-size characterization [13]; an important advantage of the volumetric method is that the adsorbent is in direct contact with the thermostat and the adsorbent temperature is well defined. The volumetric method is based on calibrated volumes and pressure measurements, and it uses the general gas equation of state. The adsorbed amount is calculated by determining the difference of the total amount of gas admitted to the sample cell with the adsorbent and the amount of gas in the dead space. In this scenario, the dead volume needs to be very accurately determined.

Physical adsorption in micropores occurs at relative pressures substantially lower (very often down to relative pressures below 10^{-5}) than in the case of adsorption in mesopores and special requirements are necessary to obtain accurate adsorption isotherms on microporous samples. The most important point is that physical adsorption in micro- and mesoporous adsorbents can span a broad spectrum of pressures (up to seven orders of magnitude). In order to study the adsorption of gases such as nitrogen and argon (at their boiling temperatures) within the relative pressure range from $10^{-7} \leq P/P_0 \leq 1$ with sufficiently high accuracy, it is desirable to use a combination of different transducers within different pressure ranges. In addition, one has to assure that the sample cell and the manifold can be evacuated to very low pressures, which requires a proper high vacuum pumping system, i.e. a turbomolecular pump. Further it is also highly recommended to monitor the saturation pressure, P_0, throughout the entire analysis that can be achieved by means of a dedicated saturation pressure transducer.

In order to obtain correct data, it is required to remove all physically adsorbed material from the adsorbent surface to ensure a reproducible initial state. In principle, this can be accomplished by vacuum pumping or purging with an inert gas at elevated temperatures. Outgassing under vacuum is desirable because it prepares the surface under the same conditions (evacuated sample cell) that are required to start a static volumetric adsorption experiment. This is particularly important for carbons with very narrow micropores; here, the adsorption measurements often start at relative pressures as low as 10^{-7}, and the samples require an outgassing at pressures below 0.01 Pa. This can be achieved by using a turbomolecular pump which, if coupled with a diaphragm roughing pump, allows the sample to be outgassed even in a completely oil-free system.

4.2.2. Choice of Adsorptive

4.2.2.1. Standard Adsorptives for Carbon Characterization

The question of which adsorptive to choose for the physical adsorption characterization is important in particular with regard to the fact that for nitrogen adsorption at 77 K, micropore filling of carbon pores smaller than 1 nm (which are present in many carbon materials) occurs at very low pressures. The rate of diffusion and adsorption equilibration is extremely slow at relative pressures below 10^{-5}. Furthermore, a pore width of 0.7 nm corresponds to the thickness of the bilayer formed by nitrogen molecules. Preadsorbed N_2 molecules near the entry of a narrow micropore may block further adsorption. This leads to time-consuming measurements and may cause under-equilibration of measured adsorption isotherms, giving erroneous results for the analysis. For characterization of microporous materials, it may be necessary to utilize other gases (such as argon or carbon dioxide) to accurately determine pore-size distributions in some carbons. Although the kinetic diameters of nitrogen (0.36 nm), argon (0.34 nm), and carbon dioxide (0.33 nm) are similar, the adsorption behavior of these three adsorptives is quite different.

Argon at 87 K shows nearly perfect adsorption behavior because, compared to nitrogen and carbon dioxide, argon does not give rise to specific interactions with a variety of surface functional groups, which can lead to enhanced adsorption/specific interactions caused by quadrupole moment characteristic to non-symmetric molecules. As a consequence of this factor and a slightly higher temperature, argon at 87 K fills micropores of dimensions 0.5–1 nm at higher relative pressures compared to nitrogen at 77 K, leading to accelerated diffusion and faster equilibration times. This effect is much more pronounced, for instance, for zeolites and metal–organic frameworks than for carbons. The pore-filling pressures of argon (87 K) are often shifted 1–1.5 decades in relative pressure as compared to nitrogen [17,18]. A comparison between argon (87 K) and nitrogen (77 K) adsorption on a physically activated carbon (obtained from Norit) is shown in Fig. 4.1 and is also discussed in detail in [19].

The question arises whether the advantages of argon adsorption at 87 K will also be present at liquid nitrogen temperature (77 K). Unfortunately, argon adsorption at 77 K is less than optimal for both pore size and surface area analysis because (i) a combined and complete micro- and mesopore size analysis with argon is not possible at 77 K (which is ca. 6.5 K below the triple point temperature of bulk argon) and is limited to pore diameters smaller than 16 nm (for details see [20]); (ii) although the argon adsorption isotherm at 77 K is still shifted to higher relative pressures as compared to the appropriate nitrogen adsorption, the shift toward higher absolute pressure is less pronounced as compared to argon adsorption at 87 K. This is due to the low saturation pressure of argon at 77 K (205 torr for solid argon and 230 torr for

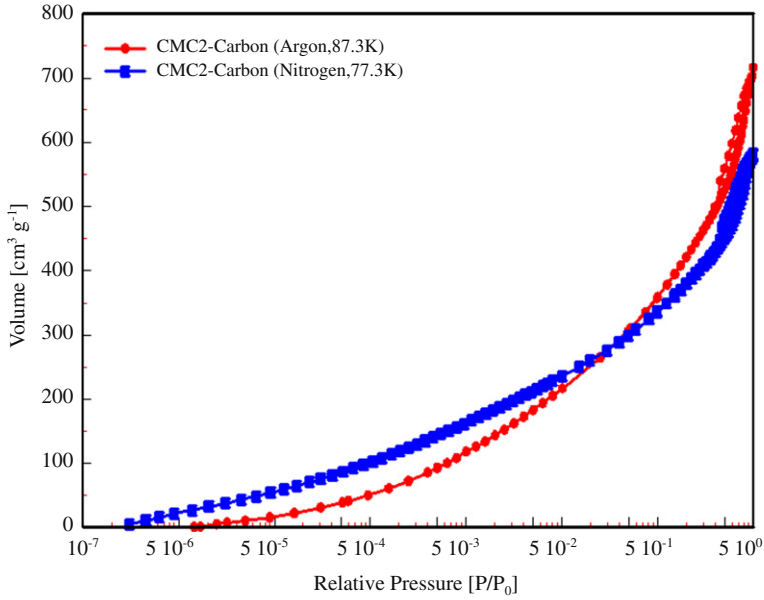

FIGURE 4.1 Nitrogen (77 K) and argon (87 K) adsorption isotherms on activated carbon.

supercooled liquid argon). Hence, argon adsorption at 77 K does not offer the same "experimental benefits" as argon adsorption at 87 K.

Despite the advantages which argon adsorption at 87 K offers, pore filling of ultramicropores still occurs at very low pressures. Associated with the low pressures is the well-known problem of restricted diffusion, which prevents nitrogen and also argon molecules from entering the narrowest micropores – pores of width <0.45 nm. In order to address this, the use of CO_2 as adsorptive at temperatures close to room temperature has been suggested. At 273 K for instance, CO_2 is still ca. 32 K below its critical temperature and because the saturation pressure is very high (26,200 torr), the relative pressure measurements necessary for the micropore analysis are achieved in the range of moderate absolute pressures (1–760 torr). Hence, due to the relatively high absolute temperatures and pressures compared with nitrogen and argon adsorption at cryogenic temperatures, it has been established that diffusion limitations of nitrogen in micropores can be eliminated by the use of CO_2 [21–23]. CO_2 molecules are able to easily access the ultramicropores despite the fact that the dimensions of N_2, Ar, and CO_2 are similar. Furthermore, the experimental setup needed to perform micropore analysis with CO_2 is much simpler than the corresponding experimental setup for micropore analysis by argon or nitrogen adsorption, because a turbomolecular pump and low-pressure transducers are not necessary. Because of these experimental advantages, CO_2 adsorption has become a standard tool for the assessment of microporous

carbons. Consequently, advanced DFT and grand canonical Monte Carlo (GCMC) methods have been developed for calculating the pore-size distribution from the CO_2 adsorption isotherm (more details found below) [24,25].

One of the main advantages for performing CO_2 adsorption experiments at 273 K is that, because of the enhanced kinetics, a micropore characterization with CO_2 can be performed in few hours – much faster than adsorption experiments at cryogenic temperatures. However, it should be noted that in particular for carbons with very narrow pores, as found in some carbon molecular sieves, the adsorption is sensitive to the chosen experimental equilibration parameter [26]. The kinetics of CO_2 adsorption in carbon micropores has also been investigated (for carbon aerogels) by combining adsorption experiments with small-angle X-ray scattering [27]. Additionally, similar to nitrogen, CO_2 has a quadrupole moment, which affects the adsorption behavior on carbons containing oxygen surface functionalities, complicating the pore-size analysis by CO_2 for such carbons [28].

A nice example which demonstrates the complementary use of various adsorptives along with the proper use of DFT for calculation of pore-size distribution (discussed in detail below) is shown in Fig. 4.2. Nitrogen (77 K), argon (87 K), and carbon dioxide (273 K) were used to characterize an ultramicroporous carbon (microwave-exfoliated graphene oxide) useful for supercapacitor applications [29]. Figure 4.2a shows the nitrogen, argon, and carbon dioxide isotherms on this carbon (plotted in a linear scale) and Fig. 4.2b shows the three isotherms plotted in a semi-logarithmic scale. The semi-logarithmic plots illustrate that carbon dioxide fills even the narrowest micropores at much higher relative pressures than both nitrogen and argon. In the case of this carbon, the NLDFT pore-size distribution calculated from the carbon dioxide adsorption isotherm clearly shows the presence of pores smaller than 0.7 nm (Fig. 4.2c). Only with the combination of carbon dioxide and nitrogen adsorption can complementary and complete pore-size and pore-volume information be determined. It is also worthwhile noting that the NLDFT cumulative pore-volume data (Fig. 4.2c) allows one to differentiate between micro- and mesopore volume in a straightforward manner.

4.2.2.2. Other Adsorptives for Carbon Characterization

With the recent growing interest in hydrogen storage and fuel cell applications, there has been increased research on hydrogen adsorption on carbon materials and pore-size determination using hydrogen at 77 K. Although highly supercritical at this temperature, it has been shown that by using hydrogen adsorption at 77 K coupled with a proper NLDFT approach, pore-size analysis can be extended to pore sizes smaller than those that can be characterized with other adsorptives, including CO_2 [30,31]. However, the use of hydrogen as an adsorptive for pore-size analysis is limited to a pore width range smaller than 0.5 nm.

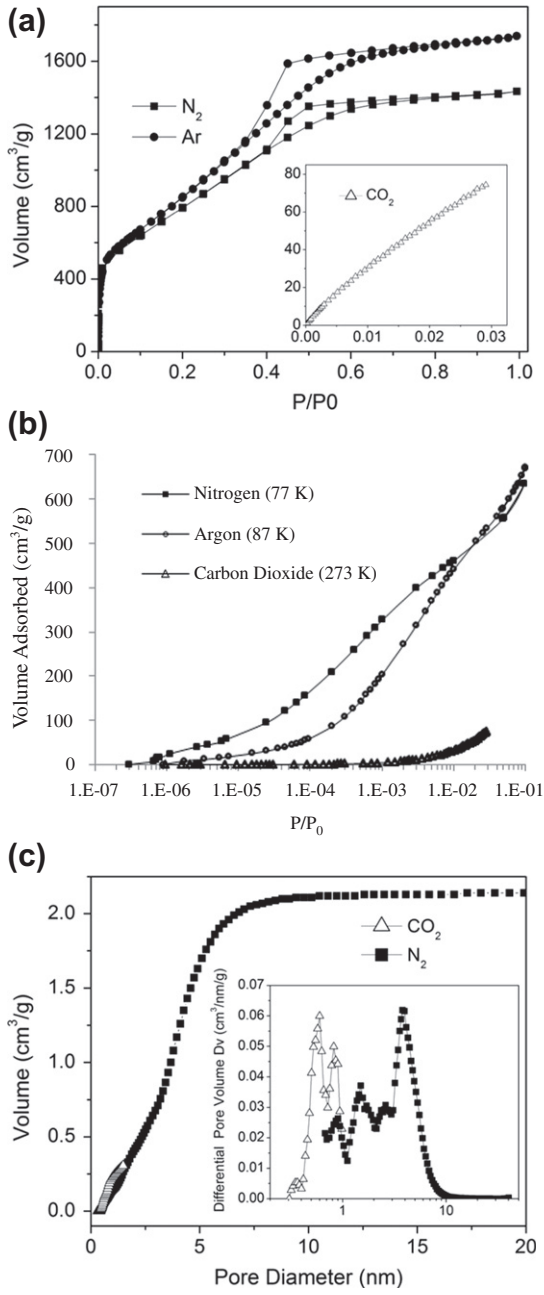

FIGURE 4.2 (a) Nitrogen (77 K) and argon (87 K) isotherms on a microwave-exfoliated graphene oxide material. Inset is the carbon dioxide (273 K) isotherm on the same material, (b) semi-logarithmic display of the nitrogen (77 K), argon (87 K), and carbon dioxide (273 K) isotherms highlighting the low-pressure adsorption data up to a relative pressure of 10^{-2}, and (c) cumulative pore-volume and (inset) pore-size distribution calculated using DFT methods. *(From [26]. Reprinted with permission from AAAS)*

The method of nonane preadsorption has been suggested many decades ago [7] for the characterization of complex micro- and mesoporous carbons. Here, one assesses microporosity by the retention of *n*-nonane in narrow pores. In this method, the narrow micropores are filled with nonane, which can only be desorbed at elevated temperatures – the narrower the micropore, the higher the temperature to remove the nonane. However, this method is not always straightforward, and in carbons which exhibit a wide pore-size distribution, nonane adsorbed in narrow micropores may block the entrances to the wider pores. Recently, *n*-nonane preadsorption has been successfully applied to lignocellulosic-derived activated carbons [32] in order to elucidate the details of their complex micro–mesopore network.

The use of water as a probe for surface chemistry and pore structure analysis has attracted a great deal of interest [33–47]. Water is an appealing adsorbtive because it can be adsorbed at room temperature and has a very small kinetic diameter (0.28 nm), which allows for probing the pores that are not accessible to nitrogen or carbon dioxide [38]. A comparison of water (at 298 K) and nitrogen (at 77 K) adsorption on purely microporous physically activated carbon TE80 (from Pica Corporation) is shown in Fig. 4.3 [48]. The isotherms are of completely different shape, type I for nitrogen adsorption (based on the IUPAC classification) but type V for water adsorption. Whereas in the case of nitrogen the micropores are already completely filled at a relative pressure <0.1, micropore filling with water occurs at relative pressures >0.4 due to the hydrophobic nature of the carbon surface. Up to this pressure, almost no

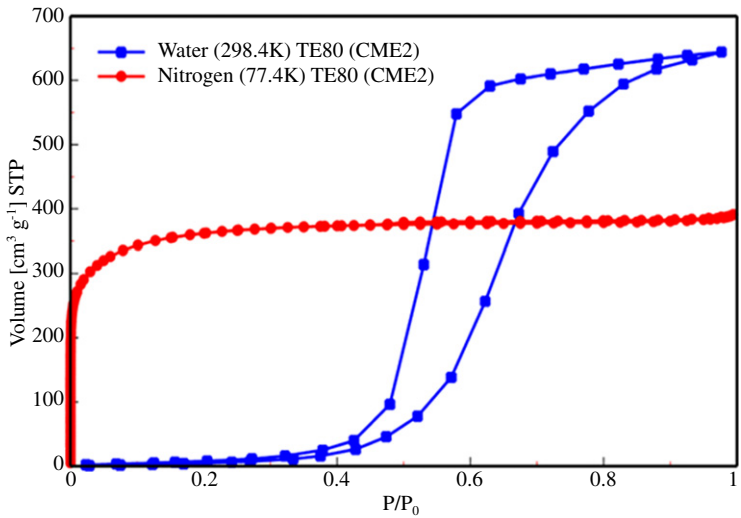

FIGURE 4.3 Comparison of nitrogen (77 K) and water (298 K) adsorption isotherms on a physically activated carbon (Picactif TE80 from Pica) illustrating the adsorption hysteresis observed for the micropores in the water isotherm. *(From [48]. Reprinted with Permission)*

adsorption was observed. Further, the water sorption isotherms show hysteresis, due to different mechanisms of adsorption/pore filling (*via* clustering) and desorption (*via* molecular evaporation), as discussed in the literature [34,46]. It should be noted that the occurrence of hysteresis in the range where nitrogen and argon isotherms are reversible can potentially be useful for textural characterization.

However, interpretation of water isotherms is difficult because of the competing effects of pore structure and surface chemistry. In a recent study, these effects were investigated for three commercially available activated carbons [48]. Water adsorption was coupled with textural analysis *via* nitrogen and argon adsorption, as well as surface characterization by TPD-MS and XPS. Although all three carbons studied had essentially identical micropore structures (as evidenced by a combination of Ar (87 K), N_2 (77 K), and CO_2 (273 K) adsorption), differences in the water adsorption isotherms could be clearly associated with differences in surface chemistry, indicating the potential of water adsorption for surface chemistry assessments.

In order to assess the smallest pore dimensions in microporous materials, Kaneko et al. suggested helium which is the smallest inert molecule [49,50]. Of course, the experiments have to be performed below helium's critical temperature (ca. 5.2 K) and Kaneko et al. measured helium adsorption at 4.2 K on activated carbon fibers. From these data, micropore volumes 20–50% greater than those obtained from nitrogen adsorption at 77 K were found. The excess amount of helium adsorption was ascribed to the presence of ultramicropores, which cannot be accessed by nitrogen molecules.

4.3. ADSORPTION MECHANISM

In order to obtain surface area, pore-size distribution, pore volume, and other structural information from the analysis of gas adsorption isotherms, it is necessary to understand the underlying adsorption mechanisms. The mechanisms of micro- and mesopore filling differ substantially. The filling of micropores is, in most cases, a continuous process. The filling of ultramicropores occurs at low relative pressures ($P/P_0 < 0.01$) and is entirely governed by the enhanced gas–solid interactions. However, in addition to the strong adsorption potential, a cooperative mechanism may play a role in the pore-filling process of supermicropores ($P/P_0 \approx 0.01$–0.2). The relative pressure, at which the micropore filling occurs, depends on a number of factors, including the size and nature of adsorptive molecules, pore shape, and effective pore width. The pore-filling capacity depends essentially on the accessibility of the pores for the probe molecules, which is determined by the molecular size and chosen experimental conditions. A basic understanding of the micropore-filling process has already been achieved by Dubinin and co-workers based on the pioneering work of Polanyi [51,52].

By contrast, mesopores fill *via* capillary condensation, which represents a gas–liquid phase transition. The sorption behavior in mesopores depends not only on the fluid–wall attraction, but also significantly on the attractive interactions between the adsorbate molecules. This leads to the occurrence of multilayer adsorption and capillary condensation. Capillary condensation represents a phenomenon whereby gas condenses to a liquid-like phase in pores at a pressure less than the saturation pressure, P_0, of the bulk fluid. It represents an example of a shifted bulk transition under the influence of the attractive fluid–wall interactions. Capillary condensation is very often accompanied by hysteresis, and it is widely accepted that there is a correlation between the shape of the hysteresis loop and the texture of the adsorbent. An empirical classification of hysteresis loops was given by IUPAC [13].

Traditionally, pore condensation has been described within the Kelvin approach [see Refs. 7–9 and references therein]. For pores of uniform shape and width (ideal slit-like or cylindrical mesopores), the shift of the gas–liquid-phase transition of a confined fluid from bulk coexistence is expressed in terms of the macroscopic quantities like the surface tension of the bulk fluid, the densities of the coexistent liquid, and the contact angle of the liquid meniscus against the pore wall. However, the Kelvin concept fails to correctly describe the peculiarities of the critical region, confinement-induced shifts of the phase diagram of condensed fluid, and hysteresis behavior, specifically the disappearance of hysteresis with decreasing pore size (at given temperature) or increasing temperature (for a given pore size) (for a review see [12,53]).

By contrast, it has been shown that modern, microscopic approaches such as DFT (NLDFT and QSDFT) and molecular simulation (grand canonical Monte Carlo (GCMC) simulation) are capable of qualitatively and quantitatively predicting capillary condensation and hysteresis behavior of fluids in highly ordered model materials. Two principal factors determine the hysteretic behavior: hysteresis on the level of a single pore of given shape and the cooperative effects due to the specifics of pore network connectivity. On the pore level, adsorption hysteresis is considered as an intrinsic property of the vapor–liquid phase transition in a finite volume system. A classical scenario of capillary condensation implies that the vapor–liquid transition is delayed due to the existence of metastable adsorption films and hindered nucleation of liquid bridges. In open, uniform cylindrical pores of finite length, metastable states occur only on the adsorption branch. In an open pore filled by liquid-like condensate, the liquid–vapor interface is already present and evaporation occurs without nucleation, *via* a receding meniscus. That is, the desorption process is associated with the equilibrium vapor–liquid transition. This mechanism of adsorption hysteresis is present in ordered mesoporous materials with uniform cylindrical pores (e.g. MCM-41, SBA-15). In order to describe hysteresis phenomena in more disordered adsorbents, network models have been developed [54–60]. The network models attribute hysteresis to pore-blocking/percolation effects.

In the case of pore blocking, in a material with an ink-bottle shape pore, desorption is delayed and the wide body of the pore remains filled until the neck evaporates at a lower vapor pressure. Additionally, the desorption branch of the hysteresis loop is significantly steeper than the adsorption branch, resulting in a hysteresis loop of type H2 according to the IUPAC classification. Adsorption/desorption mechanisms were recently studied with the aid of model materials containing well-defined ink-bottle pores (e.g. SBA-16, hierarchically ordered porous materials such as KLE) [61–67]. These theoretical and experimental studies revealed that if the pore neck diameter is smaller than a certain critical size at a given temperature and adsorptive, desorption occurs *via* cavitation, or spontaneous nucleation of a bubble in the pore. In this case, the pore body empties, while the pore neck remains filled. Figure 4.4 illustrates that for a given temperature and adsorptive, the neck size dictates the desorption mechanism. In the case of pore blocking (neck width larger than the critical width of ca. 5–6 nm for nitrogen and argon adsorption at 77 and 87 K, respectively), evaporation occurs at the equilibrium pressure of the corresponding meniscus and, therefore, information about the neck (pore entrance size) can be obtained from the desorption branch of the isotherm. In the case where the neck is smaller than the critical size, desorption from the pore body occurs *via* cavitation. Studies of the temperature dependence of the hysteresis loop in such materials showed a transition between cavitation and pore-blocking regimes, suggesting a possibility of

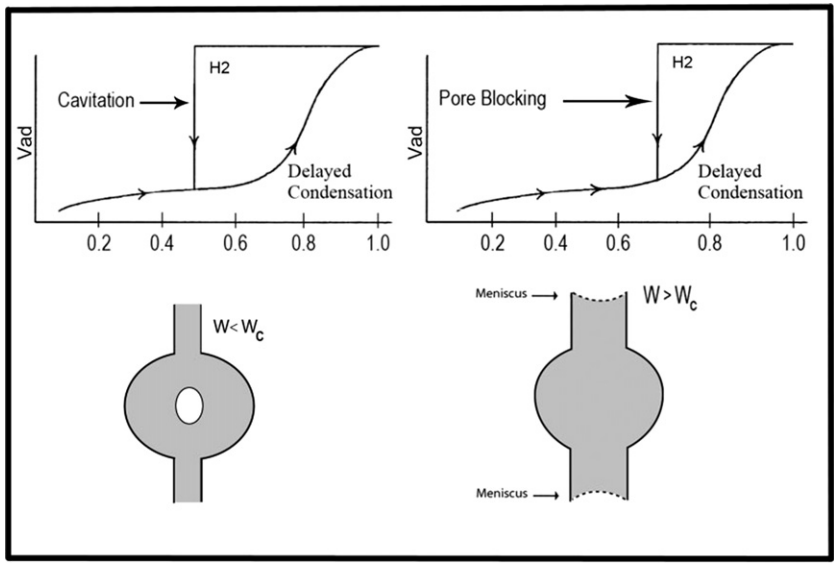

FIGURE 4.4 Schematic of pore-blocking and cavitation phenomena. W is the size of the pore neck and W_c is the critical neck size below which cavitation is the desorption mechanism. *(Reprinted with Permission from [69]. Copyright 2006 American Chemical Society)*

estimating the neck-size distribution from the desorption isotherm by tuning the experimental conditions [64]. Another possibility is to use various probe molecules and it has been demonstrated that adsorption experiments performed with two adsorptives (e.g. nitrogen and argon at 77 K and 87 K, respectively) allow for detecting and separating the effects of pore-blocking/percolation and cavitation [67].

Cavitation-induced evaporation appears to be important for many micro- and mesoporous solids and is responsible for the often observed characteristic stepdown in the desorption isotherm at relative pressure ranges from 0.4 to 0.5 (giving rise to type H3 and H4 hysteresis). In the past, this characteristic stepdown was discussed within the framework of the tensile strength hypothesis [7,68] which was associated with the lower closure point of hysteresis. In this classical approach, it was supposed that the tensile stress limit of condensed fluid, which is indicated by cavitation, does not depend on the nature and pore structure of the adsorbent, but is a universal feature of the adsorptive. However, the observed cavitation-induced stepwise desorption in ink-bottle pores occurs at appreciably larger pressures (up to relative pressures of 0.5) than the "universal" lower closure point of hysteresis mentioned above, which for nitrogen (at 77 K) and argon (at 87 K) was assumed to be at relative pressures of 0.42 and 0.38, respectively. Although there is a weak dependency of the cavitation pressure on the pore size for pore diameters smaller than ca. 12 nm (for spherical pores) [69], the position of the cavitation transition is mainly determined by the state of the pore fluid. Hence, pore-size analysis from the desorption isotherm would lead to artificial spikes around a pore size of 4 nm (for reviews, see [11,12]).

4.4. ASPECTS OF SURFACE AREA ASSESSMENT

Surface area is the crucial parameter for optimized porous carbons for many applications. However, due to the complex nature of micro- and mesoporous materials, no single experimental technique can be expected to provide an evaluation of the "absolute" surface area. Surface area values are of relative nature and should always be related to the method, conditions, and probe molecules used in the experimental work. Despite the well-known limitations, the Brunauer–Emmett–Teller (BET) method continues to be widely used for the evaluation of surface areas of micro- and mesoporous adsorbents. The BET equation is applicable for the surface area estimates of nonporous, macro-, and mesoporous materials (pore width > 4 nm), but its extension to microporous materials contradicts the basic physical mechanism of micropore volume filling rather than monolayer coverage implied by the BET theory [8,9]. In the case of microporous materials, the surface area obtained using the BET method should be considered as an "equivalent" surface area. Despite this limitation, the BET method is the most frequently used method for surface area determination of porous carbons.

In order to determine the BET surface area, one must first transform the measured isotherm into a BET plot from which the monolayer capacity, n_m, is derived. Once the monolayer capacity has been determined, the surface area can be calculated using the molecular cross-sectional area. The monolayer capacity, n_m, is calculated using the BET equation:

$$\frac{p/p_0}{n_a[1-(p/p_0)]} = \frac{1}{n_m C} + \frac{C-1}{n_m C}\cdot\frac{p}{p_0}$$

where n_a is the adsorbed amount and C is an empirical constant that gives an indication of the attractive adsorbent–adsorbate interactions. Emmett and Teller originally found that various adsorbents gave linear BET plots over the relative pressure range $P/P_0 = 0.05$–0.3.

In microporous materials, micropores fill at relative pressures below 0.1 and it is difficult to separate monolayer formation from micropore filling. The linear BET range is often shifted to significantly lower relative pressures, but the problem of which relative pressure range should be chosen for BET analysis is of prominent importance because of the possibility for significant overestimation of the monolayer capacity. In order to address the problem, Rouquerol et al. have determined a procedure for finding the linear BET range for a microporous material [70,117]. Based on an alternative plotting of the BET equation first proposed in 1961 [71], they suggest that (a) C must be positive (i.e. any negative intercept on the BET plot indicates that one is outside the valid range of the BET equation) and (b) application of the BET equation must be limited to the range where the term $[V(1-P/P_0)]$ continuously increases with P/P_0. This method has recently been adopted by the International Organization for Standardization (ISO) (ISO FDIS 9277, Determination of the Specific Surface Area of Solids by Gas Adsorption BET Method, 2009) and is successful at accurately determining the linear BET range for microporous materials. This method is illustrated with the example of a microporous activated carbon fiber (ACF) sample in Fig. 4.5. If the traditional linear BET pressure range is applied to the data, the resulting BET plot (Fig. 4.5a) is nonlinear, indicating an incorrect BET plot/range. Additionally, the BET plot intercept is negative, meaning that the C-constant is negative as well, which is unphysical. In this case, the calculated BET area is 1008 m^2/g. If, instead, the method of Rouquerol et al. is applied, a plot such as the one shown in Fig. 4.5b results. The maximum of this plot indicates the highest relative pressure in the linear BET range. This information is used to construct the linear BET plot in Fig. 4.5c. As such, a linear BET range of 0.026–0.071, well below the range recommended for mesoporous materials, is found, corresponding to the "equivalent" BET area of 1167 m^2/g, over 100 m^2/g more than if the traditional BET range is used.

In order to address problems associated with applying the BET equation to microporous materials, it was also suggested to treat the physisorption data of nitrogen by a modified BET equation, which includes the micropore volume,

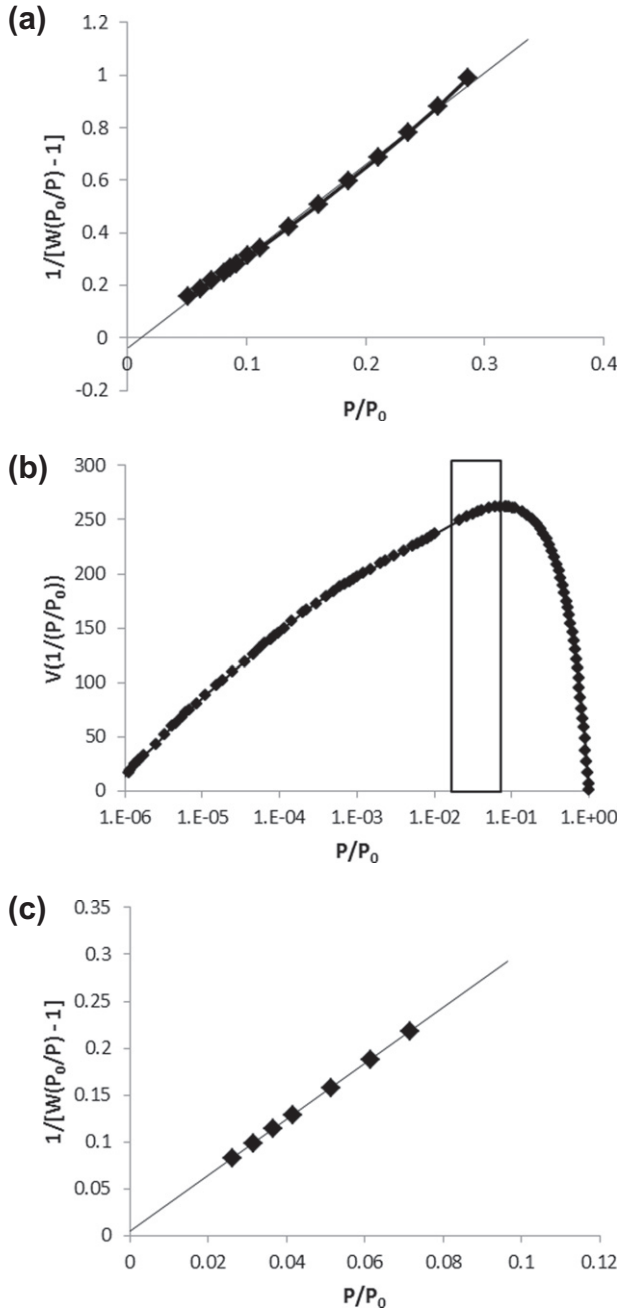

FIGURE 4.5 (a) BET plot for an activated carbon fiber sample using the classical relative pressure range ($P/P_0 - 0.05$–0.3), (b) plot of P/P_0 vs. $V(1 - P/P_0)$ used to determine the upper limit (graph maximum) for the BET range, and (c) BET plot in the relative pressure range determined using the method proposed by Rouquerol et al.

V_{micro}. The suggested approach allows one to extract the V_{micro} value from the adsorption data and consequently to determine the value of C_{BET} and specific surface area of the nonmicroporous part of the sample [72]. Other methods to obtain a specific surface area from gas adsorption are based on the application of the standard isotherm concept, e.g. *t*- and alpha-s methods which allow one to obtain the external (nonmicroporous) surface area [7–9]. By subtracting the external surface area from the BET area, one can determine a micropore surface area. A micropore surface area can also be obtained by methods related to the Dubinin approach (i.e. the Dubinin–Kaganer method) [7–9].

Another alternative to obtain the surface area of microporous solids and to differentiate between micro- and external surface area is the application of the DFT method, which calculates the specific cumulative surface area (specific surface area as a function of pore size) over the complete range of micro- and mesopores. However, accurate results are obtained only if the given experimental adsorptive/adsorbent system is compatible with one of the available DFT methods. Details of the DFT methods are discussed below.

A recent study of 190 different porous carbons confirmed that the application of the BET method is problematic for assessing surface areas [73]. It was suggested that the application of methods derived from the Dubinin-Radushkevitch approach, methods based on density functional theory (NLDFT and QSDFT), and the application of immersion calorimetry are useful concerning the surface area determination of microporous carbons.

4.5. PORE SIZE AND POROSITY ANALYSIS

4.5.1. General Comments

As indicated before, over the last two decades tremendous progress has been achieved with regard to the understanding of sorption phenomena in narrow pores, which in turn led to major progress in physical adsorption characterization. This progress is greatly associated with the development and application of microscopic methods, such as the density functional theory (DFT) of inhomogeneous fluids (e.g. nonlocal density functional theory, NLDFT) or computer simulation methods (e.g. Monte Carlo (MC) and molecular dynamic (MD) simulations) [53,74–83]. These molecular-level methods, which are based on statistical mechanics, describe the specifics of distribution of adsorbed molecules in pores, in contrast to the classical methods which are based on macroscopic, thermodynamic assumptions (e.g. Dubinin–Radushkevich (DR), Horvath–Kawazoe (HK), comparison plot methods for the analysis of micropores, or Kelvin equation-based methods such as the Barrett–Joyner–Halenda (BJH) or Broekhoff–de Boer (BDB) methods for analysis of mesopores) [7–9]. Each of these classical methods is based on the assumption of a certain adsorption mechanism within a pore width range (i.e. micro- or mesopores) and, consequently, one needs to combine at least two methods for

characterization of porous carbons which contain both micro- and mesopores. On the other hand, application of a DFT-based method allows one to obtain a reliable pore-size analysis over the complete micro- and mesopore-size range.

4.5.2. Classical, Macroscopic Thermodynamic and Empirical Methods for Pore Size and Porosity Analysis

4.5.2.1. Micropore Analysis

In the absence of mesoporosity, the physisorption isotherm is of type I (according to the IUPAC classification) with a plateau which is virtually horizontal. In this case, one can correlate the adsorbed amount in the plateau region directly with the micropore volume by applying the Gurvitsch rule [84]. The Gurvitsch rule implies that the pores are filled with a homogeneous, bulk-like liquid, an assumption that does not account for the fact that the degree of molecular packing in small pores depends on both the pore size and shape. This problem has been addressed by applying microscopic methods (e.g. molecular simulation or DFT), which reflect the degree of molecular packing in the details of the density profile.

In order to assess the micropore volume (and average pore width) of nanoporous carbons, methods based on the Dubinin–Radushkevich (DR) approach [52,85] are frequently applied; the DR method is still considered a standard tool for obtaining micropore volume. The DR equation is written as follows:

$$V_a = V_{micro}\exp\left[-\left\{\left(\frac{RT}{\beta E_o}\right)\ln\frac{p_0}{p}\right\}^2\right]$$

where V_a is the volume of liquid adsorbate, V_{micro} is the micropore volume, β is the affinity coefficient (e.g. 0.33 for nitrogen), and E_0 is the characteristic adsorption energy. A plot of $\log V_a$ vs. $[\log(P_0/P)]^2$ should give a straight line, which is very often found at relative pressures between 10^{-4} and 10^{-2}. The volume of mesopores, V_{meso}, is then estimated by subtracting V_{micro} from the total pore volume, which is obtained from the Gurvitsch rule at a relative pressure where all pores are filled (typically at $P/P_0 = 0.95$).

The DR equation often fails to linearize the data when the microporous adsorbent is very heterogeneous with regard to surface chemistry and texture. To overcome such deficiencies in the original DR equation, a more general equation, known as the DA equation, was proposed by Dubinin and Astakhov [86]. Another generalization of the DR equation has been introduced by Stoeckli et al. [87,88]. Based on empirical studies, Dubinin and Stoeckli proposed that E_0 can be related to the average micropore width, W, for a carbonaceous adsorbent by the following simple formula: $W = 26$ (kJ nm/mol)/E_0. Later, Stoeckli et al. [89,90] suggested a slightly modified relationship: $W = 13.7$ (kJ nm/mol)/$(E_0 - 9.7)$. More recent work focused on the

influence of carbon surface oxygen groups on the DA equation parameters for CO_2 adsorption on carbons [29].

It is also worthwhile to note that within this context the relationship between the pore volumes and surface areas derived from nitrogen adsorption isotherms using several different methods (DR, BET, and t-plot) has been recently investigated [91]. Carbon aerogels exposed to temperatures varying from 1000 °C to 2500 °C were used as model materials and a linear correlation was observed between the BET surface area and the DR pore volume.

Furthermore, the application of the standard and comparison isotherm concept allows one to determine micropore volume, (external) surface area, and, in principle, information about the average pore size. The t-plot method proposed by Lippens and de Boer [92] compares the test isotherm on a microporous material with a reference type II isotherm composed of averaging the experimental data on a number of nonporous adsorbents with a BET C constant similar to that of the microporous sample being tested. The experimental test isotherm is then redrawn as a *t*-curve, i.e. a plot of the volume of gas adsorbed as a function of *t*, which is the standard multilayer thickness on the reference nonporous material at the corresponding P/P_0. Another method for estimating micropore volume is the alpha-s method, developed by Sing et al. [93,94]. An advantage compared to the *t*-method is that the construction of the alpha-s plot does not require the monolayer capacity and allows, therefore, for a more direct comparison between the test isotherm and the reference isotherm (for details, see [7]). The reference isotherm in the alpha-s method is a plot of the amount of gas adsorbed, normalized by the amount of gas adsorbed at a fixed relative pressure vs. P/P_0. The reference relative pressure is usually taken as $P/P_0 = 0.4$, and the normalized $V_{ads}/V_{ads}^{0.4}$ is plotted. Principally, the alpha-s method allows one to (i) identify the physisorption mechanisms; (ii) check the validity of the BET nitrogen area; (iii) evaluate the total surface area of nonporous or mesoporous solids; and (iv) assess the effective micropore volume and external area of an ultramicroporous or supermicroporous solid. It is also worthwhile mentioning that Kaneko et al. [95] introduced the high-resolution alpha-s analysis, based on a high-resolution standard isotherm. The high-resolution method makes particular use of the alpha-s plot below $P/P_0 = 0.4$ and allows one to obtain more information concerning micro- and mesoporosity in the adsorbent.

A more advanced method, which allows for the determination of the micropore-size distribution of microporous carbons up to a pore width of 2 nm, was put forward by Horvath and Kawazoe (HK) and is based on the work of Everett and Powl [96,97]. The HK method allows for the calculation of the micropore-volume distribution from a low-pressure nitrogen adsorption isotherm obtained on a slit-pore carbon. Saito and Foley extended this approach to argon (87 K) adsorption in zeolitic pores with cylindrical pore geometry [98]. Contrary to the classical, Dubinin-related approaches, the HK approach employs the adsorption potential in slit carbon pores and provides a detailed

account for the enhancement of the adsorption potential as the pore-size decreases. The advantage of the HK method is that it is specific with respect to the pore shape and adsorbate–adsorbent interaction potential. However, a disadvantage is that it does not give a realistic description of the micropore filling because it neglects the inhomogeneity of the adsorbed molecules in the micropores, leading to inaccuracies in the pore size and volume determination. Some improvements of the HK method have been considered [99], but treatments such as DFT or methods of molecular simulation are superior and provide a much more accurate approach for pore-size analysis over the complete range of micro- and mesopores.

4.5.2.2. Mesopore Analysis

The Kelvin equation serves as the basis for many methods of mesopore analysis, including the widely used Barrett–Joyner–Halenda (BJH) method. The Kelvin equation provides a relationship between the pore diameter and the pore condensation pressure and predicts that pore condensation shifts to a higher relative pressure with increasing pore diameter and temperature. In order to account for the multilayer adsorbed film, the Kelvin equation is combined with a standard isotherm (i.e. *t*-curve), which usually refers to the adsorption on a reference nonporous solid. The Kelvin equation is written as

$$\ln(P/P_0) = -2\gamma \cos\theta/\mathrm{RT}\Delta\rho(r_\mathrm{p} - t_\mathrm{c})$$

where R is the universal gas constant, r_p the pore radius, and t_c is the thickness of an adsorbed multilayer film, which is formed prior to the capillary condensation. For nitrogen and argon adsorption at their boiling temperatures (77.4 K and 87.3 K, respectively), the contact angle, θ, of the adsorbate adsorbed on the pore walls is zero (i.e. situation of complete wetting).

The multilayer adsorbed film is assessed by the statistical (mean) thickness of an adsorbed film on a nonporous solid of a surface similar to that of the sample under consideration. However, it is obvious that assuming the situation of a nonporous, planar surface for the evaluation of the adsorbed film thickness cannot be valid in the case of narrow pores, where the curvature of the pore walls and their adsorption potential has a pronounced effect on the film thickness and its interfacial tension. The validity of the Kelvin equation also becomes questionable because it does not allow for the effect of the adsorption forces on the pore condensation. Furthermore, the macroscopic, thermodynamic concept of a smooth liquid–vapor interface and bulk-like core fluid cannot be realistically applied to condensation in narrow mesopores. The development of model mesoporous molecular sieves (e.g. M41S materials) allowed for the first time direct experimental tests of the validity of the modified Kelvin equation and the BJH method. Because of the high degree of order, the pore diameter of such model substances can be derived by independent methods

(X-ray-diffraction, high-resolution transmission electron microscopy, etc.). It was found that the BJH method and related procedures underestimate the pore size by up to 20–30 % for pores smaller than 10 nm if not properly corrected. Some improvement was achieved by modifying the classical Broekhoff–de Boer approach and by calibrating the Kelvin equation using a series of mesoporous molecular sieves (MCM-silicas) of known pore diameter [118,119]. However, it needs to be stressed that approaches based on calibration are strictly only valid over a limited pore-size range (for reviews, see [11,12]). On the contrary, as discussed in the following section, advanced methods based on density functional theory (DFT) and molecular simulation allow one to obtain an accurate pore-size analysis and combined micro- and mesopore analysis. This is also demonstrated in Fig. 4.6 which shows the pore-filling pressure for nitrogen (77 K) in slit-pore carbons as predicted by DFT, Horvath Kawazoe (HK), and modified Kelvin equation (MK) for a series of pore widths [75]. For a given pore-filling pressure, the corresponding micropore width, as predicted by the HK method (micropore range) and modified Kelvin equation (mesopore range), is underestimated compared to the prediction by DFT.

4.5.3. Modern, Microscopic Methods for Pore Size and Porosity Analysis: Density Functional Theory

DFT and computer simulation methods (such as molecular dynamics and Monte Carlo simulation) are powerful techniques that describe sorption and phase

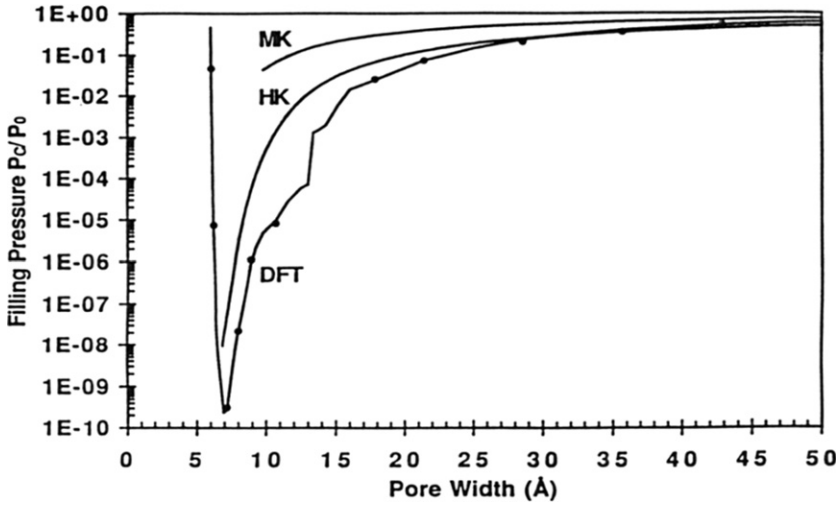

FIGURE 4.6 Pore-filling pressures for nitrogen (77 K) in slit-pore carbons as a function of pore width as predicted by DFT, HK, and modified Kelvin (MK) equations. *(Reprinted with Permission from [75]. Copyright 1993 American Chemical Society)*

behavior of inhomogeneous fluids confined in nanoporous materials [74–83]. These approaches describe the distribution of adsorbed molecules in pores and thus provide detailed information about the local fluid structure near curved solid walls as compared to the bulk fluid structure. It is generally assumed that at experimental conditions the adsorbate in a pore is in thermodynamic equilibrium with a bulk gas phase. The local density, $\rho(r)$, of the pore fluid is therefore determined by minimization of the grand thermodynamic potential, which depends on the intermolecular potentials of fluid–fluid (adsorbate–adsorbate) and fluid–solid (adsorbate–adsorbent) interactions, whereby the latter depends on the pore geometry. The parameters of the fluid–fluid interactions are usually determined in a way that they reproduce the bulk fluid properties (e.g. surface tension and gas–liquid coexistence curve). The parameters of the solid–fluid potential are chosen to fit the standard adsorption isotherms on well-defined nonporous carbon material. Once $\rho(r)$ is known, other thermodynamic properties, such as the adsorption isotherm, energy of adsorption, and positions of phase transitions, can be calculated.

Pioneering studies on DFT and the adsorption and phase behavior of fluids in pores were performed by Evans and Tarazona [100,101]. Seaton et al. [81] were the first to apply DFT for the calculation of the pore-size distribution (PSD) in both the meso- and micropore ranges. In this first attempt, the pore-size distribution analysis based on the local version of DFT was used. Although the local DFT provides a qualitatively reasonable description of adsorption in pores, it is quantitatively inaccurate especially in the range of micropores. A significant improvement in accuracy was obtained with the nonlocal density functional theory (NLDFT), which was first reported for the pore-size analysis of microporous carbons in 1993 [75]. Since then, NLDFT has been frequently used for the pore-size analysis of micro- and mesoporous materials (for a review, see [10] and references therein) and the NLDFT method is now commercially available for many adsorbent/adsorptive systems.

A drawback of the NLDFT method for the pore-size characterization of disordered carbon materials is that the solid surface is treated as molecularly smooth and its predictions imply pronounced layering steps on adsorption isotherms, which are not observed in experimental adsorption isotherms on amorphous carbons. This can cause prominent artifacts in the NLDFT PSDs, such as the gap at ca. 1 nm, which is characteristic of many porous-activated carbons [24,102]. Several approaches have been suggested to account for the heterogeneity of carbon materials including the development of advanced structural models of porous carbons by reverse Monte Carlo techniques [1,78,80] which, however, are still too complex to be implemented for routine pore-size analyses. Others suggested modeling porous carbons with a mixed geometry model [103]. Molecular simulations have also demonstrated that the surface roughness and defects significantly affect the shape of adsorption isotherms on heterogeneous surfaces [35,104–106].

Within the framework of the standard slit-pore model of carbons, variability of pore-wall thickness was introduced [107,108], but it led to just a marginal improvement over the standard NLDFT approach. The drawbacks of the conventional NLDFT model were also addressed by the introduction of two-dimensional DFT approaches [109].

In order to account quantitatively for the effects of surface heterogeneity in a practical way, the quenched solid density functional theory (QSDFT) was introduced. In contrast to the conventional NLDFT models that assume structureless graphitic pore walls, the solid is modeled using the distribution of solid atoms rather than the source of the external potential field. Within the framework of QSDFT, the grand potential of both solid and fluid is considered. In fact, QSDFT is a multicomponent DFT, in which the solid is treated as one of the components of the adsorbate–adsorbent system. The surface heterogeneity in the QSDFT model is characterized by a single roughness parameter that represents the characteristic width of molecular level surface corrugations. It has been demonstrated that the QSDFT model significantly improves the method of adsorption porosimetry [15,19]. The QSDFT method for carbons [15] has originally been developed assuming slit-shaped pores, which are typical model pores in activated microporous carbons. However, due to the emergence of novel materials with predesigned pore morphology obtained by synthesis routes which make use of structure directing agents or hard templates, the QSDFT method has recently been extended to micro–mesoporous carbons with cage-like and channel-like pore geometries [16].

In this chapter, we do not focus on the theoretical and mathematical details of the NLDFT and QSDFT methods, which were described in detail in [75,110] for NLDFT and in [15,16] for QSDFT. The calculation of the pore-size distribution is based on a solution of the *generalized adsorption equation* (GAE) which is sometimes also called *integral adsorption equation*, as given in the equation below, which correlates the kernel of theoretical adsorption (or desorption) isotherms with the experimental adsorption (desorption) isotherm:

$$N_{\mathrm{exp}}(P/P_0) = \int_{D_{\mathrm{min}}}^{D_{\mathrm{max}}} N_{\mathrm{QSDFT}}(P/P_0, D) f(D) \mathrm{d}D$$

Here, D_{min} and D_{max} are the minimum and maximum pore sizes in the kernel. The kernel $N_{\mathrm{QSDFT}}(P/P_0, D)$ represents a set of theoretical isotherms in model pores for a series of pore diameters, which cover the whole range of micro- and mesopores accessible in the adsorption experiment.

The kernel can be regarded as a theoretical reference for a given class of adsorbent/adsorptive systems. A typical QSDFT kernel of theoretical isotherms of nitrogen (77 K) adsorption in cylindrical carbon pores is shown in Fig. 4.7 [16].

The experimental isotherm is represented as the convolution of the DFT kernel (set of the theoretical isotherms) in a series of pores within a given range of pore sizes, D, and the sought pore-size distribution function $f(D)$. The procedure is illustrated schematically in Fig. 4.8.

Solution of the GAE equation is obtained using the quick non-negative least-squares method [110]. In this method, the equation is represented as a matrix equation, which is solved using the discrete Tikhonov regularization method combined with the non-negative least-squares algorithm.

As mentioned before, the standard NLDFT approaches do not sufficiently take into account the chemical and geometrical heterogeneity of the pore walls and a structureless, molecularly smooth pore-wall model is assumed. This mismatch between the theoretical NLDFT assumptions and the experimental systems causes the theoretical adsorption isotherms to exhibit multiple steps associated with layering transitions related to the formation of a monolayer, second adsorbed layer, and so on. These layering steps on the theoretical isotherms can cause artificial gaps on the calculated pore-size distributions. Figure 4.9 illustrates this problem for nitrogen (77 K) adsorption on activated carbon fiber (ACF-15). The prominent step at $P/P_0 = 0.3 \times 10^{-3}$, which is characteristic of the theoretical NLDFT isotherms and is due to the monolayer transition on the smooth graphite surface, is completely eliminated in the QSDFT isotherm. As a consequence, a sharp minimum in the NLDFT pore-size

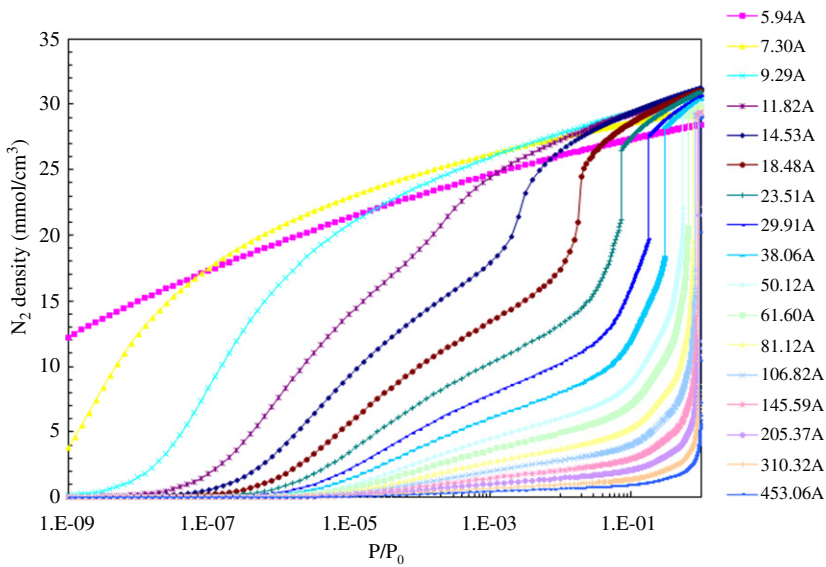

FIGURE 4.7 Kernel of adsorption isotherms of nitrogen at 77 K in cylindrical pores with molecularly rough walls. The pore widths are given in the right panel. *(Reprinted from [16], with Permission from Elsevier)*

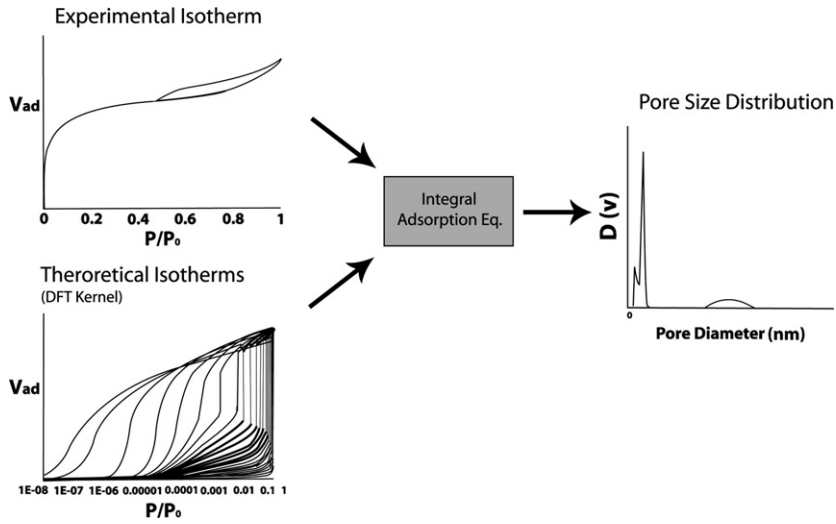

FIGURE 4.8 Schematic representation of the procedure applied to calculate a DFT pore-size distribution from experimental adsorption/desorption isotherms.

distribution curve at ~1 nm, which is typical to the NLDFT pore-size distribution curves for many microporous carbons, does not appear in QSDFT calculations. This confirms that the minimum on the differential NLDFT pore-size distribution is indeed an artifact caused by the monolayer step in the NLDFT approach. The pore-size distribution curves in Fig. 4.9b show that QSDFT and NLDFT agree above and below the regions where artificial gaps were observed with NLDFT; this is in line with the observation that the cumulative pore-volume curves calculated by NLDFT and QSDFT (Fig. 4.9c) are also in good agreement [15] outside the 1-nm pore width range.

A similar scenario is observed for argon (87 K) adsorption. Pore-size distributions calculated using the argon QSDFT methods likewise do not exhibit the layering transition characteristic of NLDFT and any false minima in the pore-size distribution, as shown for a Calgon F400 activated carbon in Fig. 4.10.

4.5.4. Pore-Size Characterization of Micro–Mesoporous Carbon Materials – Selected Application Examples

In order to validate and test recently developed QSDFT methods for cylindrical carbon pores, ordered mesoporous carbon CMK-3, which is an inverse replica of SBA-15 silica [111], has been employed. The complete micro- and mesopore-size distribution of ordered CMK-3 was calculated from both the adsorption and desorption branches of the nitrogen (77 K) isotherm (Fig. 4.11a) by applying a N_2 (77 K) cylindrical pore carbon QSDFT method to both the

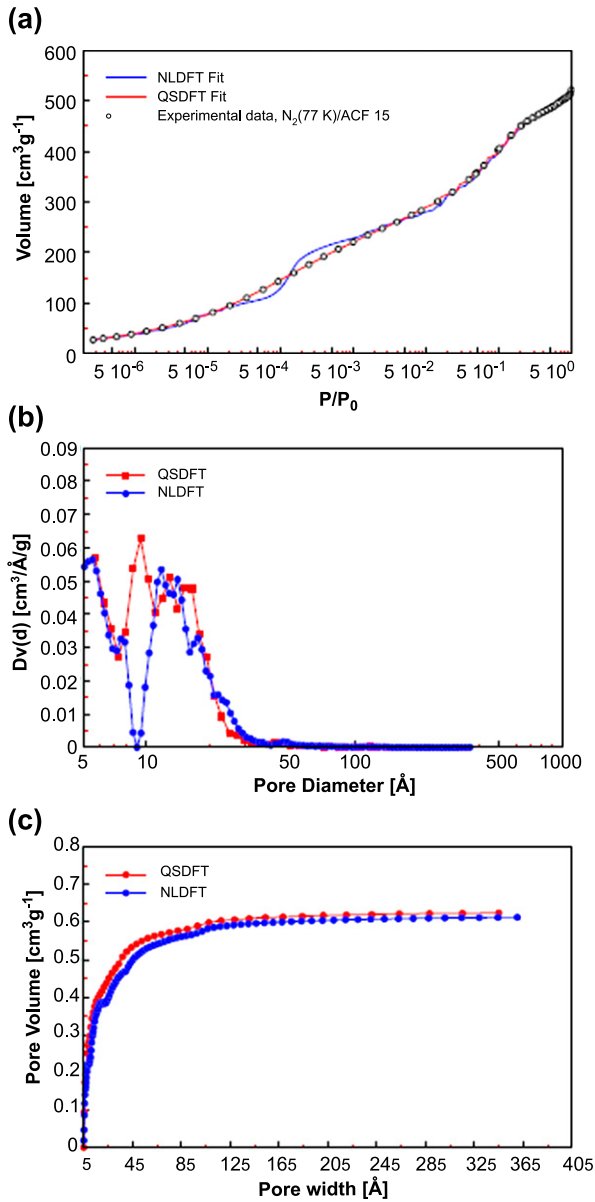

FIGURE 4.9 Comparison of the NLDFT and QSDFT methods for nitrogen (77 K) adsorption on activated carbon fiber ACF-15. (a) Experimental isotherm plotted on a semi-logarithmic scale with the NLDFT and QSDFT theoretical isotherms, (b) NLDFT and QSDFT pore-size distributions calculated from the nitrogen isotherm, and (c) QSDFT and NLDFT cumulative pore volumes. *(Reprinted from [15], with Permission from Elsevier)*

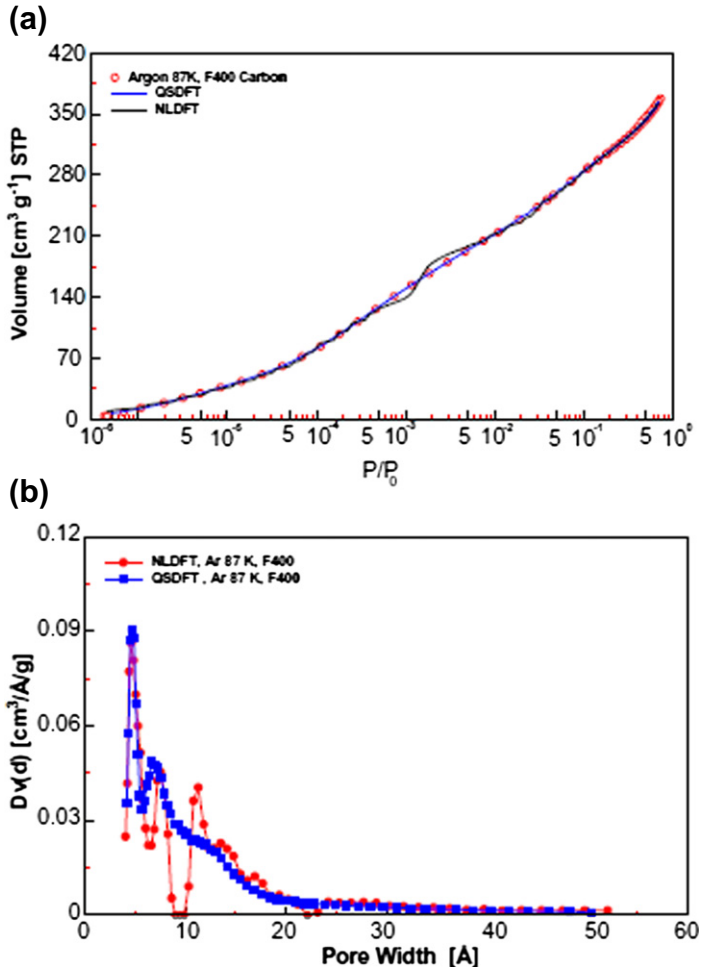

FIGURE 4.10 Pore-size distributions calculated for granular-activated carbon Calgon F400. (a) Experimental argon (87 K) isotherm plotted on a semi-logarithmic scale together with the NLDFT and QSDFT theoretical isotherms and (b) NLDFT and QSDFT pore-size distributions calculated from the argon isotherm. *(Reprinted from [15], with Permission from Elsevier)*

adsorption and desorption data (Fig. 4.11b). An excellent fit of the QSDFT model to both the adsorption branch and desorption branch (Fig. 4.11a) of the experimental isotherm is obtained by applying (i) the adsorption branch kernel,

FIGURE 4.11 Nitrogen (77 K) adsorption on a CMK-3 sample. (a) Experimental isotherm with fit-from-QSDFT cylindrical adsorption and cylindrical equilibrium kernels, (b) pore-size distributions from QSDFT cylindrical adsorption and cylindrical equilibrium kernels derived from adsorption and desorption branches of the experimental isotherm, and (c) pore-size distributions calculated from the nitrogen isotherm using the BJH and QSDFT methods.

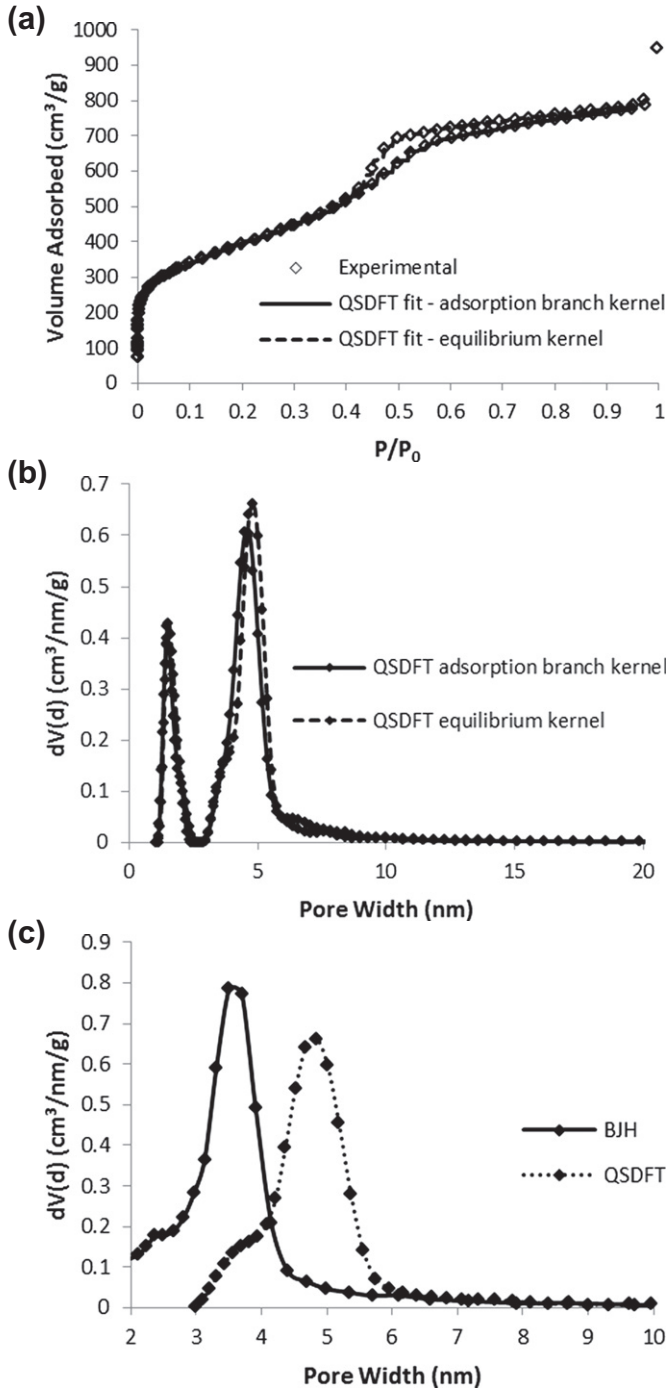

which takes correctly into account the delay in condensation due to metastable pore fluid in the region of hysteresis, to the adsorption data and (ii) the equilibrium QSDFT kernel on the desorption data. Overlapping pore-size distributions were observed, indicating that, for this particular sample, the desorption branch essentially represents evaporation under equilibrium conditions, i.e. hysteresis is here essentially caused by metastable pore fluid due to the existence of metastable adsorption films associated with the pore condensation. The obtained QSDFT mean mesopore diameter (4.8 nm) agrees well with the pore size derived from a geometrical model of CMK-3 (assuming hexagonally arranged carbon rods according to [112]) coupled with X-ray diffraction data (5 nm) obtained on this sample confirming that the QSDFT method accurately calculates the pore size from the experimental data [16].

Figure 4.11c compares the QSDFT mesopore-size distribution of this CMK-3 sample with the prediction of the BJH method. The BJH pore-size distribution curve is shifted significantly (ca. 25 %) to lower pore size, similar to the results obtained for silica mesoporous molecular sieves [11,12] and confirming that macroscopic, thermodynamic methods not only fail to provide a pore-size distribution over the complete micro- and mesopore range but also have a tendency to underestimate the pore size even in the range where they can be applied. This is further demonstrated in Fig. 4.12 which shows the micropore-size distributions calculated using the HK and QSDFT methods from a nitrogen adsorption isotherm obtained on a typical activated carbon sample (Fig. 4.12a). The HK pore-size distribution is shifted to smaller pore widths as compared to the QSDFT pore-size distribution, which is expected (see Fig. 4.6 which compares pore-filling pressures for nitrogen (77 K) in slit-pore carbons as a function of pore width as predicted by DFT, HK, and modified Kelvin (MK) equations).

Furthermore, novel QSDFT hybrid methods assuming cylindrical pore geometry for micro- and narrow mesopores, but spherical pore geometry for pores of width larger than 5 nm were applied to study the pore-size distribution of novel three-dimensionally ordered mesoporous (3DOm) carbons [16]. Here, good agreement with pore-size results from independent methods has also been found.

The combination of various adsorptives (argon and nitrogen) coupled with a proper QSDFT method allows us to obtain information about pore morphology and pore topology of complex micro–mesoporous carbons, as it has recently been demonstrated for the characterization of lignocellulosic-derived activated carbons [32]. Figure 4.13a shows argon (87 K) and nitrogen (77 K) isotherms on such samples with a type H3/H4 hysteresis loop indicating clearly the presence of complex meso- and microporosity. As discussed earlier, the use of different adsorptives, such as nitrogen and argon, allows one to identify and separate the underlying adsorption and hysteresis mechanisms. By comparing the pore-size distribution curves obtained from the argon and nitrogen desorption branches, one can differentiate whether pore blocking/percolation or cavitation-induced evaporation occurs, which provides

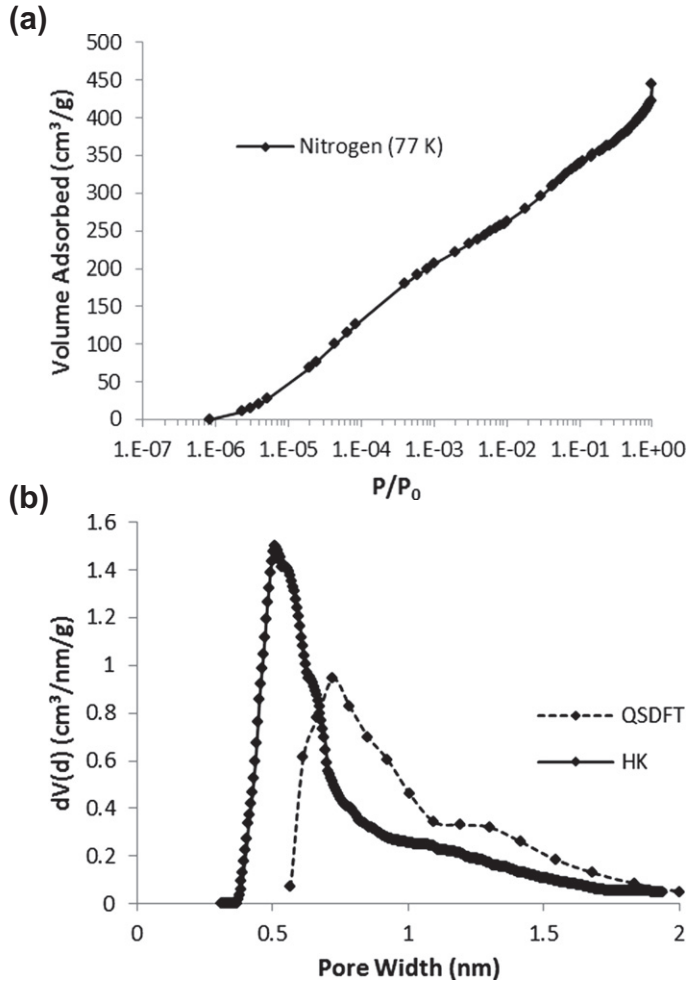

FIGURE 4.12 (a) Nitrogen (77 K) sorption isotherm for a microporous-activated carbon and (b) pore-size distributions calculated from the nitrogen isotherm using the HK and QSDFT methods.

additional information about pore network properties. It is interesting to note that the argon and nitrogen pore-size distribution curves from the desorption branches agree well for the mesopores with diameters up to 4 nm, but then deviate significantly for the pore-size range between ca. 4 and 6 nm (Fig. 4.13b). In line with our discussion of adsorption mechanism, this indicates that the steps down in the desorption branches around $P/P_0 = 0.4$ are associated with cavitation-induced evaporation from larger mesopores, which are only accessible by pore entrances with widths smaller than ca. 5–6 nm. In this case, no further quantitative information about the size of the necks can be obtained from the desorption pore-size distributions, and the argon and nitrogen

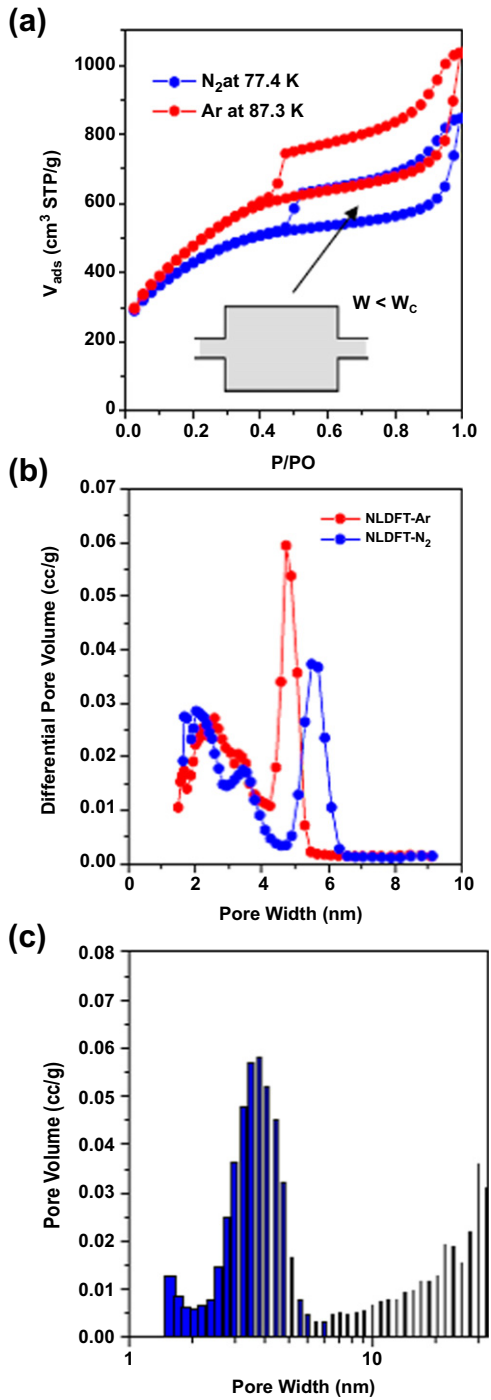

FIGURE 4.13 (a) Nitrogen (77 K) and argon (87 K) adsorption–desorption isotherms for a lignocellulosic-derived carbon. Inset shows a schematic representation of the large mesoporous cavities connected to the external surface through narrower mesopore necks, (b) pore-size distributions calculated from the desorption branches of the nitrogen and argon isotherms using NLDFT (assuming a cylindrical pore model), and (c) pore-size distribution calculated from the adsorption branch using a QSDFT metastable adsorption branch model (assuming a slit/cylindrical pore model). *(Reprinted from [32], with Permission from Elsevier)*

pore-size distribution peaks in this region reflect an artificial pore-size distribution. An accurate pore-size distribution of this material could only obtained from the adsorption branch by applying a QSDFT model to the nitrogen data which takes into account delay of condensation due to metastable pore fluid in cylindrical carbon mesopores. This distribution is shown in Fig. 4.13c in the form of a histogram, clearly indicating that this sample consists of a bimodal

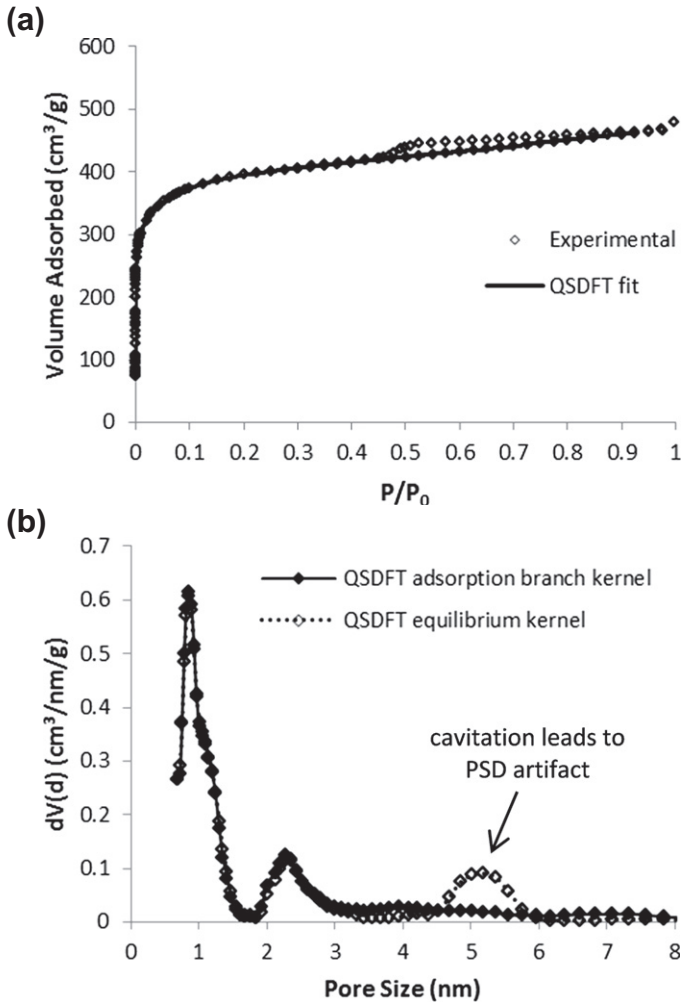

FIGURE 4.14 (a) Carbide-derived carbon nitrogen (77 K) adsorption isotherm with QSDFT fit and (b) pore-size distribution calculated from the desorption branch using a QSDFT equilibrium kernel illustrating the artifact due to cavitation at around 5 nm and pore-size distribution calculated from the adsorption branch using a QSDFT metastable adsorption branch kernel.

mesopore-size distribution, whereby some of the larger mesopores are only accessible by significantly smaller entrances.

Another interesting example is given in Fig. 4.14 which shows the nitrogen (77 K) adsorption isotherm of a typical carbide-derived carbon [113,114]. The isotherm reveals a type H4 hysteresis loop indicating the presence of micro- and mesopores. The steep stepdown in the isotherm around a relative pressure of 0.4 indicates the presence of cavitation in this sample. In this case, an accurate pore-size distribution must be calculated from the adsorption branch of the isotherm. Hence, a hybrid QSDFT method which assumes slit-pore geometry for the micropores and a cylindrical pore model to describe correctly the adsorption/condensation mechanism in the mesopores, i.e. takes into account the delay in condensation due to metastable adsorption fluids, was applied. Figure 4.14a demonstrates that this model fits the experimental adsorption isotherm and the resulting pore-size distribution is shown in Fig. 4.14b. In addition, the pore-size distribution was obtained from the desorption branch by applying a slit/cylinder QSDFT equilibrium transition model. The obtained pore-size distribution agrees with the pore-size distribution derived from the adsorption branch with the exception of the artificial peak at 5 nm which is due to cavitation-induced evaporation, indicating that some larger pores are only accessible through necks/entrances which are smaller than a critical width (around 5–6 nm for N_2/77 K adsorption).

4.6. CONCLUSIONS

During recent years, major progress has been achieved in the understanding of adsorption and phase behavior in ordered micro- and mesoporous materials, leading to major advances in structural characterization by physical adsorption, including the development of advanced theoretical procedures based on statistical mechanics known as density functional theory (NLDFT or QSDFT) and molecular simulation (GCMC and MD). Methods such as these describe the configuration of adsorbed molecules on a molecular level, and their application has contributed to a better quantitative description of adsorption hysteresis. In certain cases, it is now possible to obtain reliable information from both the adsorption and desorption branches of the hysteresis loop, which is crucial for pore-size characterization of carbons consisting of an interconnected micro–mesoporous network. It has been demonstrated that the application of DFT-based methods provides a much more accurate and comprehensive pore-size analysis compared to macroscopic thermodynamic methods (e.g. Kelvin equation, BJH, and Horvath–Kawazoe), i.e. pore-size and pore-volume information can be obtained over the complete micro- and mesopore range. However, some classical methods, such as the Dubinin–Raduskevich-based approaches, allow one to obtain reliable micropore volumes (in agreement with DFT results). Furthermore, the recently developed QSDFT approach quantitatively accounts for surface heterogeneity effects,

providing a reliable pore-size assessment of disordered micro- and mesoporous carbons. Coupling such advanced theoretical approaches with a combination of adsorption experiments with various adsorptives (carbon dioxide, argon, and nitrogen) not only leads to a complete micro- and mesopore-size distribution, but also suggests useful information about pore morphology and topology. More work is needed to further advance the assessment of surface chemistry of nanoporous carbons by physical adsorption. It is also of interest to investigate and quantify the effects of adsorption-induced carbon pore deformation and the resulting challenges for physical adsorption characterization [115,116].

ACKNOWLEDGMENT

We would like to thank Prof. Stefan Kaskel for providing a carbide-derived carbon sample, Prof. Michael Froeba for CMK-3 mesoporous carbon, and Prof. Catherine Morlay for CMC2 activated carbon.

REFERENCES

[1] T.J. Bandosz, M.J. Biggs, K.E. Gubbins, Y. Hattori, T. Iiyama, K. Kaneko, J. Pikunic, K. Thomson, Molecular models of porous carbons, Chem. Phys. Carbon 28 (2003) 41–228.
[2] T.J. Mays, Active carbon fibers, in: Carbon Materials for Advanced Technologies, Elsevier, 1999.
[3] G.M. Roy, Activated Carbon Applications in the Food and Pharmaceutical Industries, CRC Press, 1995.
[4] H. Marsh, F. Rodríguez-Reinoso, Activated Carbon, Elsevier, 2006.
[5] F. Rodríguez-Reinoso, The role of carbon materials in heterogeneous catalysis, Carbon 36 (1998) 159–175.
[6] J. Rouquerol, D. Avnir, C.W. Fairbridge, D.H. Everett, J.H. Haynes, N. Pernicone, J.D.F. Ramsay, K.S.W. Sing, K.K. Unger, Recommendations for the characterization of porous solids, Pure Appl. Chem. 66 (1994) 1739–1758.
[7] S.J. Gregg, K.S.W. Sing, Adsorption, Surface Area and Porosity, Academic Press, 1982.
[8] F. Rouquerol, J. Rouquerol, K. Sing, Adsorption by Powders and Porous Solids, Elsevier, 1999.
[9] S. Lowell, J.E. Shields, M.A. Thomas, M. Thommes, Characterization of Porous Solids and Powders: Surface Area, Pore Size and Density, Springer, 2004.
[10] A.V. Neimark, K.S.W. Sing, M. Thommes, Surface area and porosity, in: Handbook of Heterogeneous Catalysis, Wiley, 2008.
[11] M. Thommes, Physical adsorption characterization of nanoporous materials, Chem. Ing. Tech. 82 (2010) 1059–1073.
[12] M. Thommes, Physical adsorption characterization of ordered and amorphous mesoporous materials, in: Nanoporous Materials Science and Engineering, World Scientific, 2004.
[13] K.S.W. Sing, D.H. Everett, R.A.W. Haul, L. Moscou, R.A. Pierotti, J. Rouquérol, T. Siemieniewska, Reporting physisorption data for gas/solid systems with special reference to the determination of surface area and porosity, Pure Appl. Chem. 57 (1985) 603–619.

[14] P.I. Ravikovitch, A.V. Neimark, Density functional theory model of adsorption on amorphous and microporous silica materials, Langmuir 22 (2006) 11171–11179.
[15] A.V. Neimark, Y. Lin, P.I. Ravikovitch, M. Thommes, Quenched solid density functional theory and pore size analysis of micro-mesoporous carbons, Carbon 47 (2009) 1617–1628.
[16] G.Y. Gor, M. Thommes, K.A. Cychosz, A.V. Neimark, Quenched solid density functional theory method for characterization of mesoporous carbons by nitrogen adsorption, Carbon 50 (2012) 1583–1590.
[17] M. Thommes, Textural characterization of zeolites and ordered mesoporous materials by physical adsorption, Stud. Surf. Sci. Catal. 168 (2007) 495–523.
[18] D. Lässig, J. Lincke, J. Moellmer, C. Reichenbach, A. Moeller, R. Gläser, G. Kalies, K.A. Cychosz, M. Thommes, R. Staudt, H. Krautscheid, A microporous copper metal-organic framework with high H_2 and CO_2 adsorption capacity at ambient pressure, Angew. Chem. Int. Ed. 50 (2011) 10344–10348.
[19] J. Silvestre-Albero, A. Silvestre-Albero, F. Rodríguez-Reinoso, M. Thommes, Physical characterization of activated carbons with narrow microporosity by nitrogen (77.4 K), carbon dioxide (273 K) and argon (87.3 K) adsorption in combination with immersion calorimetry, Carbon (2012). doi: 10.1016/j.carbon.2011.09.005.
[20] M. Thommes, R. Köhn, M. Fröba, Sorption and pore condensation behavior of nitrogen, argon, and krypton in mesoporous MCM-48 silica materials, J. Phys. Chem. B 104 (2000) 7932–7943.
[21] J. Garrido, A. Linares-Solano, J.M. Martín-Martínez, M. Molina-Sabio, F. Rodríguez-Reinoso, R. Torregrosa, Use of N_2 vs. CO_2 in the characterization of activated carbons, Langmuir 3 (1987) 76–81.
[22] D. Cazorla-Amorós, J. Alcañiz-Monge, A. Linares-Solano, Characterization of activated carbon fibers by CO_2 adsorption, Langmuir 12 (1996) 2820–2824.
[23] J. García-Martínez, D. Cazorla-Amorós, A. Linares-Solano, Further evidences of the usefulness of CO_2 adsorption to characterise microporous solids, Stud. Surf. Sci. Catal. 128 (2000) 485–494.
[24] P.I. Ravikovitch, A. Vishnyakov, R. Russo, A.V. Neimark, Unified approach to pore size characterization of microporous carbonaceous materials from N_2, Ar, and CO_2 adsorption isotherms, Langmuir 16 (2000) 2311–2320.
[25] A. Vishnyakov, P.I. Ravikovitch, A.V. Neimark, Molecular level models for CO_2 sorption in nanopores, Langmuir 15 (1999) 8736–8742.
[26] R.V.R.A. Rios, J. Silvestre-Albero, A. Sepúlveda-Escribano, M. Molina-Sabio, F. Rodríguez-Reinoso, Kinetic restrictions in the characterization of narrow microporosity in carbon materials, J. Phys. Chem. C 111 (2007) 3803–3805.
[27] G. Reichenauer, Micropore adsorption dynamics in synthetic hard carbons, Adsorption 11 (2005) 467–471.
[28] S. Furmaniak, A.P. Terzyk, P.A. Gauden, P.J.F. Harris, P. Kowalczyk, The influence of carbon surface oxygen groups on dubinin-astakhov equation parameters calculated from CO_2 adsorption isotherm, J. Phys. Condens. Matter 22 (2010) 085003.
[29] Y. Zhu, S. Murali, M.D. Stoller, K.J. Ganesh, W. Cai, P.J. Ferreira, A. Pirkle, R.M. Wallace, K.A. Cychosz, M. Thommes, D. Su, E.A. Stach, R.S. Ruoff, Carbon-based supercapacitors produced by activation of graphene, Science 332 (2011) 1537–1541.
[30] J. Jagiello, M. Thommes, Comparison of DFT characterization methods based on N_2, Ar, CO_2, and H_2 adsorption applied to carbons with various pore size distributions, Carbon 42 (2004) 1227–1232.

[31] J. Jagiello, W. Betz, characterization of pore structure of carbon molecular sieves using DFT analysis of Ar and H_2 adsorption data, Microporous Mesoporous Mater. 108 (2008) 117–122.
[32] A. Silvestre-Albero, M. Gonçalves, T. Itoh, K. Kaneko, M. Endo, M. Thommes, F. Rodríguez-Reinoso, J. Silvestre-Albero, Well-defined mesoporosity on lignocellulosic-derived activated carbons, Carbon 50 (2012) 66–72.
[33] J.K. Brennan, T.J. Bandosz, K.T. Thomson, K.E. Gubbins, Water in porous carbons, Colloids Surf. A 187–188 (2001) 539–568.
[34] D.D. Do, H.D. Do, A model for water adsorption in activated carbon, Carbon 38 (2000) 767–773.
[35] D.D. Do, H.D. Do, Modeling of adsorption on nongraphitized carbon surface: GCMC simulation studies and comparison with experimental data, J. Phys. Chem. B 110 (2006) 17531–17538.
[36] K. Kaneko, Y. Hanzawa, T. Iilyama, T. Kanda, T. Suzuki, Cluster-mediated water adsorption on carbon nanopores, Adsorption 5 (1999) 7–13.
[37] T. Kimura, H. Kanoh, T. Kanda, T. Ohkubo, Y. Hattori, Y. Higaonna, R. Denoyel, K. Kaneko, Cluster-associated filling of water in hydrophobic carbon micropores, J. Phys. Chem. B 108 (2004) 14043–14048.
[38] P. Lodewyckx, E.F. Vansant, Water isotherms of activated carbons with small amounts of surface oxygen, Carbon 37 (1999) 1647–1649.
[39] P. Lodewyckx, E. Raymundo-Piñero, H. Wullens, M. Vaclavikova, F. Beguin, Water isotherms of structurally identical carbons with different amounts of surface oxygen groups, in: Proceedings of the International Carbon Conference, 2008. Nagano, Japan.
[40] J.-C. Liu, P.A. Monson, Does water condense in carbon pores? Langmuir 21 (2005) 10219–10225.
[41] J.-C. Liu, P.A. Monson, Monte Carlo simulation study of water adsorption in activated carbon, Ind. Eng. Chem. Res. 45 (2006) 5649–5656.
[42] A.M. Slasli, M. Jorge, F. Stoeckli, N.A. Seaton, Modelling of water adsorption by activated carbons: effects of microporous structure and oxygen content, Carbon 42 (2004) 1947–1952.
[43] A.M. Slasli, M. Jorge, F. Stoeckli, N.A. Seaton, Water adsorption by activated carbons in relation to their microporous structure, Carbon 41 (2003) 479–486.
[44] F. Stoeckli, A. Lavanchy, The adsorption of water by active carbons, in relation to their chemical and structural properties, Carbon 38 (2000) 475–477.
[45] A. Striolo, K.E. Gubbins, M.S. Gruszkiewicz, D.R. Cole, J.M. Simonson, A.A. Chialvo, P.T. Cummings, T.D. Burchell, K.L. More, Effect of temperature on the adsorption of water in porous carbons, Langmuir 21 (2005) 9457–9467.
[46] T. Ohba, H. Kanoh, K. Kaneko, Cluster-growth-induced water adsorption in hydrophobic carbon nanopores, J. Phys. Chem. B 108 (2004) 14964–14969.
[47] P.D. Sullivan, B.R. Stone, Z. Hashisho, M.J. Rood, Water adsorption with hysteresis effect onto microporous activated carbon fabrics, Adsorption 13 (2007) 173–189.
[48] M. Thommes, C. Morlay, R. Ahmad, J.P. Joly, Assessing surface chemistry and pore structure of active carbons by a combination of physisorption (H_2O, Ar, N_2, CO_2), XPS and TPD-MS, Adsorption 17 (2011) 653–661.
[49] H. Kuwabara, T. Suzuki, K. Kaneko, Ultramicropores in microporous carbon fibres evidenced by helium adsorption at 4.2 K, J. Chem. Soc. Faraday Trans. 87 (1991) 1915–1916.
[50] K. Kaneko, N. Setoyama, T. Suzuki, H. Kuwabara, Ultramicroporosity of porous solids by He adsorption, in: Proc. IVth Int. Conf. on Fundamentals of Adsorption, 1992. Kyoto.

[51] M. Polanyi, Über die Adsorption vom Standpunkt des Dritten Wärmesatzes, Verh. Dtsch. Phys. Ges. 16 (1914) 1012–1016.
[52] M.M. Dubinin, D.P. Timofeev, Zh. Fiz. Khim. 22 (1948) 133.
[53] L.D. Gelb, K.E. Gubbins, R. Radhakrishnan, M. Sliwinska-Bartkowiak, Phase separation in confined systems, Rep. Prog. Phys. 62 (1999) 1573–1659.
[54] G. Mason, The effect of pore space connectivity on the hysteresis of capillary condensation in adsorption–desorption isotherms, J. Colloid Interface Sci. 88 (1982) 36–46.
[55] G.C. Wall, R.J.C. Brown, The determination of pore-size distributions from sorption isotherms and mercury penetration in interconnected pores: the application of percolation theory, J. Colloid Interface Sci. 82 (1981) 141–149.
[56] A.V. Neimark, Percolation theory of capillary hysteresis phenomena and its application for characterization of porous solids, Stud. Surf. Sci. Catal. 62 (1991) 67–74.
[57] M. Parlar, Y.C. Yortsos, Percolation theory of vapor adsorption–desorption processes in porous materials, J. Colloid Interface Sci. 124 (1988) 162–176.
[58] H. Liu, L. Zhang, N.A. Seaton, Sorption hysteresis as a probe of pore structure, Langmuir 9 (1993) 2576–2582.
[59] H. Liu, N.A. Seaton, Determination of the connectivity of porous solids from nitrogen sorption measurements – III. Solids containing large mesopores, Chem. Eng. Sci. 49 (1994) 1869–1878.
[60] F. Rojas, I. Kornhauser, C. Felipe, J.M. Esparza, S. Cordero, A. Domínguez, J.L. Riccardo, Capillary condensation in heterogeneous mesoporous networks consisting of variable connectivity and pore-size correlation, Phys. Chem. Chem. Phys. 4 (2002) 2346–2355.
[61] H.-J. Woo, L. Sarkisov, P.A. Monson, Mean-field theory of fluid adsorption in a porous glass, Langmuir 17 (2001) 7472–7475.
[62] L. Sarkisov, P.A. Monson, Modeling of adsorption and desorption in pores of simple geometry using molecular dynamics, Langmuir 17 (2001) 7600–7604.
[63] P.I. Ravikovitch, A.V. Neimark, Density functional theory of adsorption in spherical cavities and pore size characterization of templated nanoporous silicas with cubic and three-dimensional hexagonal structures, Langmuir 18 (2002) 1550–1560.
[64] P.I. Ravikovitch, A.V. Neimark, Experimental confirmation of different mechanisms of evaporation from ink-bottle type pores: equilibrium, pore blocking, and cavitation, Langmuir 18 (2002) 9830–9837.
[65] A. Vishnyakov, A.V. Neimark, Monte Carlo simulation test of pore blocking effects, Langmuir 19 (2003) 3240–3247.
[66] B. Libby, P.A. Monson, Adsorption/desorption hysteresis in inkbottle pores: a density functional theory and Monte Carlo simulation study, Langmuir 20 (2004) 4289–4294.
[67] M. Thommes, B. Smarsly, M. Groenewolt, P.I. Ravikovitch, A.V. Neimark, Adsorption hysteresis of nitrogen and argon in pore networks and characterization of novel micro- and mesoporous silicas, Langmuir 22 (2006) 756–764.
[68] A. Schreiber, S. Reinhardt, G.H. Findenegg, The lower closure point of the adsorption hysteresis loop of fluids in mesoporous silica materials, Stud. Surf. Sci. Catal. 144 (2002) 177–184.
[69] C.J. Rasmussen, A. Vishnyakov, M. Thommes, B.M. Smarsly, F. Kleitz, A.V. Neimark, Cavitation in metastable liquid nitrogen confined to nanoscale pores, Langmuir 26 (2010) 10147–10157.
[70] J. Rouquerol, P. Llewellyn, F. Rouquerol, Is the BET equation applicable to microporous adsorbents? Stud. Surf. Sci. Catal. 160 (2007) 49–56.

[71] T. Keii, T. Takagi, S. Kanetaka, A new plotting of the BET method, Anal. Chem. 33 (1961) 1965–1965.
[72] P. Schneider, Adsorption isotherms of microporous–mesoporous solids revisited, Appl. Catal. A 129 (1995) 157–165.
[73] T.A. Centeno, F. Stoeckli, The assessment of surface areas in porous carbons by two model-independent techniques, the DR equation and DFT, Carbon 48 (2010) 2478–2486.
[74] K.E. Gubbins, Theory and simulation of adsorption in micropores, in: Physical Adsorption: Experiment, Theory and Applications, Kluwer Academic Publishers, 1997.
[75] C. Lastoskie, K.E. Gubbins, N. Quirke, Pore size distribution analysis of microporous carbons: a density functional theory approach, J. Phys. Chem. 97 (1993) 4786–4796.
[76] K.E. Gubbins, Y.-C. Liu, J.D. Moore, J.C. Palmer, The role of molecular modeling in confined systems: impact and prospects, Phys. Chem. Chem. Phys. 13 (2011) 58–85.
[77] M.J. Biggs, A. Buts, Virtual porous carbons: what they are and what they can be used for, Mol. Sim. 32 (2006) 579–593.
[78] K.T. Thomson, K.E. Gubbins, Modeling structural morphology of microporous carbons by reverse Monte Carlo, Langmuir 16 (2000) 5761–5773.
[79] S.K. Jain, K.E. Gubbins, R.J.-M. Pellenq, J.P. Pikunic, Molecular modeling and adsorption properties of porous carbons, Carbon 44 (2006) 2445–2451.
[80] T.X. Nguyen, N. Cohaut, J.-S. Bae, S.K. Bhatia, New method for atomistic modeling of the microstructure of activated carbons using hybrid reverse Monte Carlo simulation, Langmuir 24 (2008) 7912–7922.
[81] N.A. Seaton, J.P.R.B. Walton, N. Quirke, A new analysis method for the determination of the pore size distribution of porous carbons from nitrogen adsorption measurements, Carbon 27 (1989) 853–861.
[82] J.P. Olivier, W.B. Conklin, M.V. Szombathely, Determination of pore size distribution from density functional theory: a comparison of nitrogen and argon results, Stud. Surf. Sci. Catal. 87 (1994) 81–89.
[83] A.V. Neimark, The method of indeterminate lagrange multipliers in nonlocal density functional theory, Langmuir 11 (1995) 4183–4184.
[84] L. Gurvich, J. Phys. Chem. Soc. Russ. 47 (1915) 805–827.
[85] M.M. Dubinin, L.V. Radushkevitch, Dokl. Akak. Nauk. SSSR 55 (1947) 331.
[86] M.M. Dubinin, V.A. Astakhov, Description of adsorption equilibria of vapors on zeolites over wide ranges of temperature and pressure, Adv. Chem. Series 102 (1971) 69–85.
[87] H.F. Stoeckli, A generalization of the dubinin-radushkevich equation for the filling of heterogeneous micropore systems, J. Colloid Interface Sci. 59 (1977) 184–185.
[88] M.M. Dubinin, H.F. Stoeckli, Homogeneous and heterogeneous micropore structures in carbonaceous adsorbents, J. Colloid Interface Sci. 75 (1980) 34–42.
[89] F. Stoeckli, E. Daguerre, A. Guillot, Correspondence, Carbon 37 (1999) 2075–2077.
[90] F. Stoeckli, M.V. López-Ramón, D. Hugi-Cleary, A. Guillot, Micropore sizes in activated carbons determined from the Dubinin–Radushkevich equation, Carbon 39 (2001) 1115–1116.
[91] C. Scherdel, G. Reichenauer, M. Wiener, Relationship between pore volumes and surface areas derived from the evaluation of N_2-sorption data by DR-, BET- and t-plot, Microporous Mesoporous Mat. 132 (2010) 572–575.
[92] B.C. Lippens, J.H. de Boer, Studies on pore systems in catalysts: V. The *t* method, J. Catal. 4 (1965) 319–323.
[93] D. Atkinson, P.J.M. Carrott, Y. Grillet, J. Rouquerol, K.S.W. Sing, in: Proc. 2nd Int. Conf. on Fundamentals of Adsorption, Engineering Foundation, 1987.

[94] P.J.M. Carrott, K.S.W. Sing, Gas chromatographic study of microporous carbons, J. Chromatogr. A 406 (1987) 139–144.
[95] K. Kaneko, C. Ishii, M. Ruike, H. Kuwabara, Origin of superhigh surface area and microcrystalline graphitic structures of activated carbons, Carbon 30 (1992) 1075–1088.
[96] D.H. Everett, J.C. Powl, Adsorption in slit-like and cylindrical micropores in the Henry's law region. A model for the microporosity of carbons, J. Chem. Soc., Faraday Trans. 1 (72) (1976) 619–636.
[97] G. Horvath, K. Kawazoe, Method for the calculation of effective pore size distribution in molecular sieve carbon, J. Chem. Eng. Japan 16 (1983) 470–475.
[98] A. Saito, H.C. Foley, Curvature and parametric sensitivity in models for adsorption in micropores, AIChE J. 37 (1991) 429–436.
[99] C.M. Lastoskie, A modified Horvath–Kawazoe method for micropore size analysis, Stud. Surf. Sci. Catal. 128 (2000) 475–484.
[100] P. Tarazona, Free-energy density functional for hard spheres, Phys. Rev. A 31 (1985) 2672–2679.
[101] P. Tarazona, R. Evans, A simple density functional theory for inhomogeneous liquids, Mol. Phys. 52 (1984) 847–857.
[102] J.P. Olivier, Improving the models used for calculating the size distribution of micropore volume of activated carbons from adsorption data, Carbon 36 (1998) 1469–1472.
[103] D.A. Soares Maia, J.C.A. de Oliveira, J.P. Toso, K. Sapag, R.H. López, D.C.S. Azevedo, C. L. Cavalcante, G. Zgrablich, Characterization of the PSD of activated carbons from peach stones for separation of combustion gas mixtures, Adsorption 17 (2011) 853–861.
[104] V.A. Bakaev, Rumpled graphite basal plane as a model heterogeneous carbon surface, J. Chem. Phys. 102 (1995) 1398–1404.
[105] A.R. Turner, N. Quirke, A grand canonical Monte Carlo study of adsorption on graphitic surfaces with defects, Carbon 36 (1998) 1439–1446.
[106] S.M.P. Lucena, C.A.S. Paiva, P.F.G. Silvino, D.C.S. Azevedo, C.L. Cavalcante, The effect of heterogeneity in the randomly etched graphite model for carbon pore size characterization, Carbon 48 (2010) 2554–2565.
[107] P.I. Ravikovitch, J. Jagiello, D. Tolles, A.V. Neimark, Extended Abstracts of Carbon Conference, Lexington, KY, 2001.
[108] S.K. Bhatia, Density functional theory analysis of the influence of pore wall heterogeneity on adsorption in carbons, Langmuir 18 (2002) 6845–6856.
[109] J. Jagiello, J.P. Olivier, A simple two-dimensional NLDFT model of gas adsorption in finite carbon pores. Application to pore structure analysis, J. Phys. Chem. C 113 (2009) 19382–19385.
[110] P.I. Ravikovitch, A. Vishnyakov, A.V. Neimark, Density functional theories and molecular simulations of adsorption and phase transitions in nanopores, Phys. Rev. E 64 (2001) 011602.
[111] S. Jun, S.H. Joo, R. Ryoo, M. Kruk, M. Jaroniec, Z. Liu, T. Ohsuna, O. Terasaki, Synthesis of new, nanoporous carbon with hexagonally ordered mesostructure, J. Am. Chem. Soc. 122 (2000) 10712–10713.
[112] S.H. Joo, R. Ryoo, M. Kruk, M. Jaroniec, Evidence for general nature of pore interconnectivity in 2-dimensional hexagonal mesoporous silicas prepared using block copolymer templates, J. Phys. Chem. B 106 (2002) 4640–4646.
[113] Y. Gogotsi, A. Nikitin, H. Ye, W. Zhou, J.E. Fischer, B. Yi, H.C. Foley, M.W. Barsoum, Nanoporous carbide-derived carbon with tunable pore size, Nat. Mater. 2 (2003) 591–594.

[114] E. Kockrick, C. Schrage, L. Borchardt, N. Klein, M. Rose, I. Senkovska, S. Kaskel, Ordered mesoporous carbide derived carbons for high pressure gas storage, Carbon 48 (2010) 1707–1717.
[115] E.A. Ustinov, D.D. Do, Effect of adsorption deformation on thermodynamic characteristics of a fluid in slit pores at sub-critical conditions, Carbon 44 (2006) 2652–2663.
[116] P. Kowalczyk, A. Ciach, A.V. Neimark, Adsorption-induced deformation of microporous carbons: pore size distribution effect, Langmuir 24 (2008) 6603–6608.
[117] F. Rouquerol, J. Rouquerol, B. Imelik, Validite de la loi B.E.T. dans le cas de l'adsorption d'azote, d'argon et de butane sur des adsorbants poreux, Bull. Soc. Chim. France (1964) 635–639.
[118] M. Kruk, M. Jaroniec, A. Sayari, Adsorption study of surface and structural properties of MCM-41 materials of different pore sizes, J. Phys. Chem. B 101 (1997) 583–589.
[119] M. Jaroniec, L.A. Solovyov, Improvement of the Kruk-Jaroniec-Sayari method for pore size analysis of ordered silicas with cylindrical mesopores, Langmuir 22 (2006) 6757–6760.